GCES OFFICE COPY
DO NOT REMOVE!

INITIATION AND FREQUENCY OF DEBRIS FLOWS IN GRAND CANYON, ARIZONA

by

Peter George Griffiths

GLEN CANYON ENVIRONMENTAL
STUDIES OFFICE

DEC 22 1995

RECEIVED
FLAGSTAFF, AZ

A Prepublication Manuscript Submitted to the Faculty of the

DEPARTMENT OF GEOSCIENCES

In Partial Fulfillment of the Requirements

For the Degree of

MASTER OF SCIENCE

In the Graduate College

THE UNIVERSITY OF ARIZONA

1 9 9 5

STATEMENT BY THE AUTHOR

This manuscript, prepared for publication in the Geological Society of America Bulletin, has been submitted in partial fulfillment of requirements for the Master of Science degree at the University of Arizona and is deposited in the Antevs Reading Room to be made available to borrowers as are copies of regular theses and dissertations.

Brief quotations from this manuscript are allowable without special permission, provided that accurate acknowledgement of source is made. Requests for permission for extended quotation from or reproduction of this manuscript in whole or in part may be granted by the head of the department, or the graduate program coordinator, when in their judgement the proposed use of the materials is in the interests of scholarship. In all other instances, however, permission must be obtained from the author.

SIGNED: _____ 12-13-95

APPROVAL BY RESEARCH ADVISORY COMMITTEE

As members of the Advisory/Research Committee, we recommend that this prepublication manuscript be accepted as fulfilling the research requirement for the degree of Master of Science.

_____ 12/13/95
Major Advisor - Victor R. Baker — Date

_____ 12/12/95
Robert H. Webb — Date

_____ 12.12.95.
Jay Quade — Date

Initiation and Frequency of Debris Flows in Grand Canyon, Arizona

Abstract

Debris flows are initiated in tributaries of the Colorado River in Grand Canyon, Arizona when intense precipitation causes failures in bedrock or colluvial wedges. These mass movements transport poorly sorted sediment, including very large boulders that form rapids at the mouths of tributaries and control the longitudinal profile of the Colorado River. Four failure mechanisms occur: bedrock failure, failure in colluvium, the "firehose effect" on unconsolidated colluvium, and combinations of these types. Using repeat photography, a binomial measure of debris-flow frequency consisting of whether or not an event had occurred in the last century was established for 149 of 529 tributaries. I used logistic regression modeling to evaluate the significance of twenty morphometric and lithologic variables in relation to debris-flow frequency.

Model results indicate that the presence of shale units, such as the Permian Hermit Shale, is the most consistent variable related to debris flows in Grand Canyon. These shales fail directly, produce rockfalls that store clay in colluvial wedges downslope, and form benches that store colluvial wedges. Shales also provide fine particles and clay minerals essential to the stability of debris flows. Other significant variables vary with large scale changes in canyon morphology. Standard morphometric measures of drainage-basin area and channel gradient, as well as the directional aspect of the river corridor, are significant in narrow, steep-sided eastern Grand Canyon. Measures of the location of source lithologies in general are significant in western Grand Canyon, which is wider, with larger, shallow-gradient drainages. Measures of geologic structure, and some standard hydrologic variables, were not significant.

Introduction

Debris flows are the primary sediment transport process in 529 tributaries of the Colorado River between Lees Ferry and Diamond Creek, Arizona (Melis and others, 1994; Fig. 1). This type of flash flood contains up to 80% sediment by weight, and moves a wide range of particles into the river, from fine clays to extremely large boulders (b-axis > 3 m). These boulders can be entrained by only the most extreme Colorado River floods, and thus form the framework of large debris fans that constrict

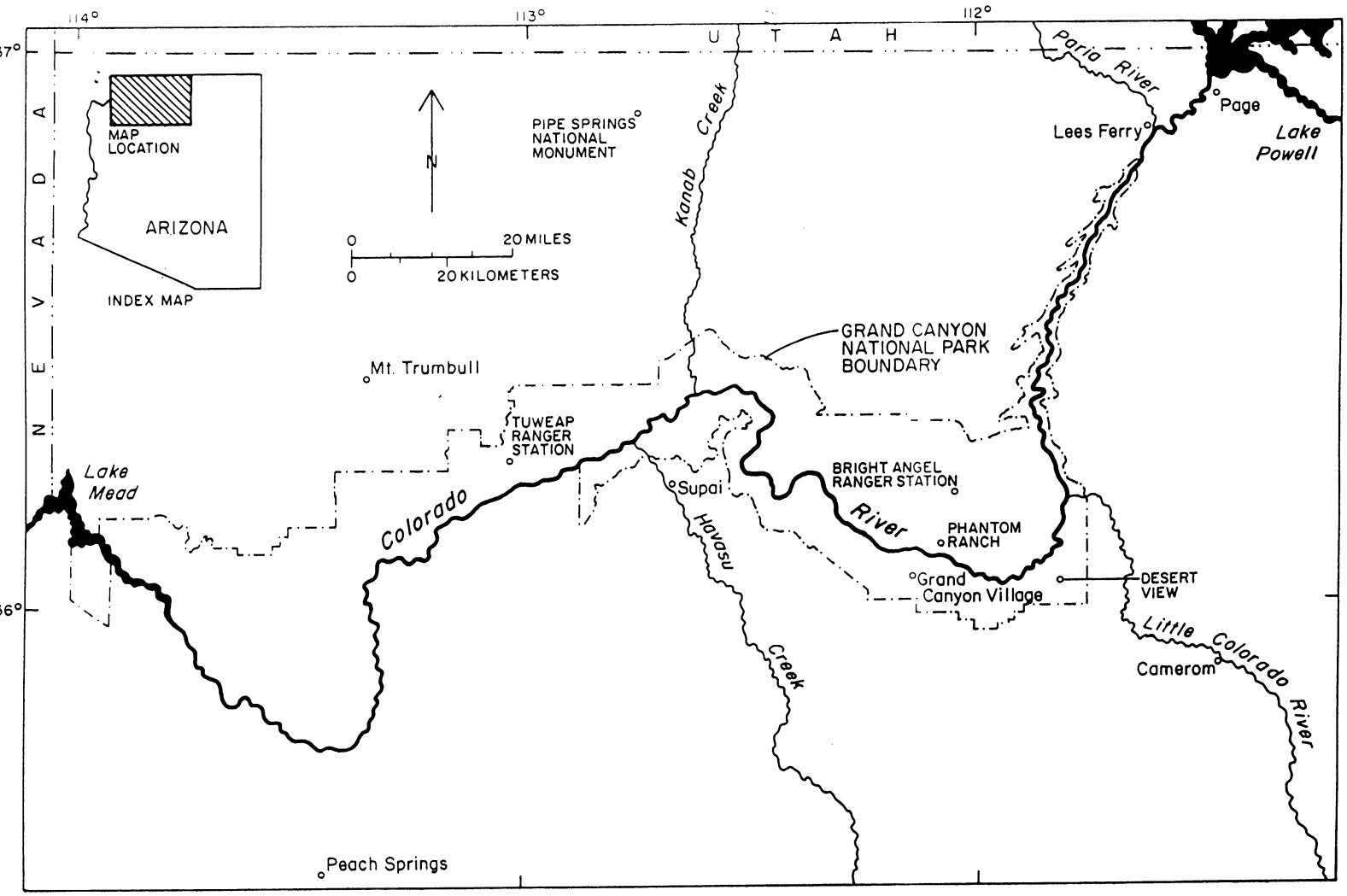

Figure 1. The Colorado River through Grand Canyon, Arizona. Circles mark precipitation gaging stations in the region.

the Colorado River at the mouths of tributary side canyons (Fig. 2). Where these deposits extend into the river, water backs up behind them in large pools and pours over in steep rapids (Hamblin and Rigby, 1968; Dolan and others, 1978; Howard and Dolan, 1981; Kieffer, 1985; Webb and others, 1989; Melis and others, 1994). Half of the vertical drop of the Colorado River occurs in these rapids, which account for only 10% of the river's length through Grand Canyon (Leopold, 1969). By forming rapids, debris flows define the longitudinal profile and control the geomorphic framework of the Colorado River in Grand Canyon.

A better understanding of the factors and processes involved in the initiation of these mass movements is critical to understanding the dynamic processes that shape and control Grand Canyon and the nation's fifth largest river. These processes are of concern not only to geomorphologists, but also to the over 20,000 white-water enthusiasts that run the rapids in Grand Canyon every summer (Stevens, 1990). An average-sized debris flow can alter the severity of a major rapid or riffle, or cover a popular camping beach with boulder-strewn debris in a matter of seconds. Fortunately, most of the Grand Canyon drainage remains wilderness that provides us with an excellent resource for studying debris flow processes that are little influenced by human activity. Moreover, the unique scenic beauty of the canyon has generated an enormous body of photographic coverage reaching as far back as 1872. These photographs contain a wealth of information on debris flows over the last century, and have allowed us to establish a substantial record of debris flow frequency over the last hundred years.

This study examines the process of debris-flow initiation in Grand Canyon, presenting field observations on the roles of climate, canyon lithology, geologic structure, and drainage-basin morphometrics. Particular emphasis is given to the roles of intense precipitation and shale source areas exposed high above river level. In order to evaluate the relative importance of various drainage-basin parameters in generating debris flows, these parameters are quantified as independent variables, and their relation to debris-flow frequency is modeled using logistic regression. Frequency measures for 149 drainages derive from techniques of repeat photography, which are used in replicating and analyzing hundreds of historical photographs taken of the river corridor during the last century. Debris-flow occurrence/non-occurrence for the last hundred years is determined by analyzing the differences between historical

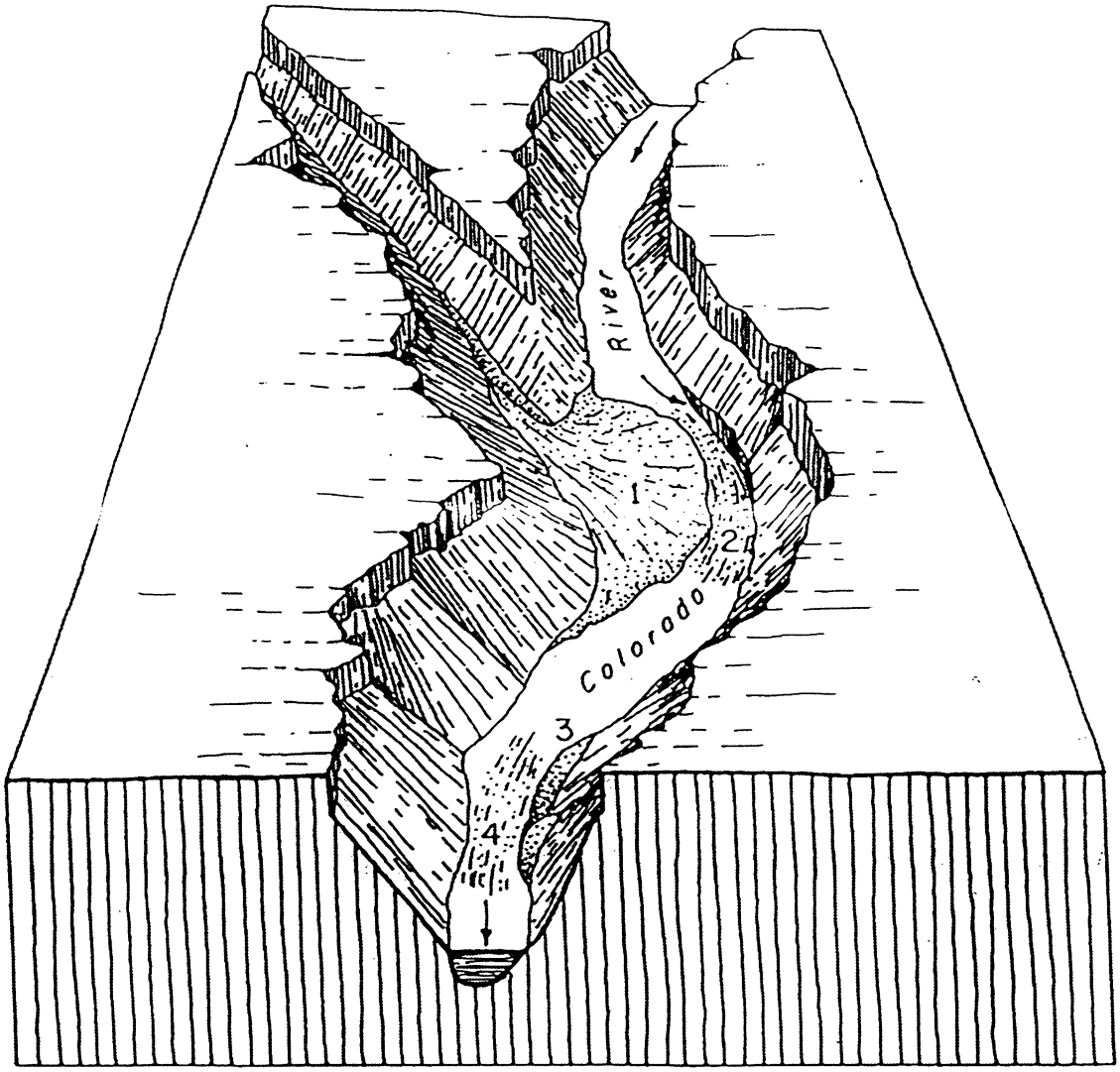

(Modified from Hamblin and Rigby, 1968)

Explanation

1. Tributary debris fan
2. Rapid controlled by large immobile boulders
3. Debris bar (synonymous with "island" or "rock garden")
4. Riffle or rapid caused by debris bar

Figure 2. The morphology of a typical debris fan and rapid of the Colorado River in Grand Canyon, Arizona.

TABLE 1. MEAN PRECIPITATION LEVELS AND TEMPERATURES AT GRAND CANYON, ARIZONA

	River Level		South Rim	North Rim
Station	Lees Ferry	Phantom Ranch	Grand Canyon	Bright Angel
Elevation (m)	978	783	2068	2560
Precipitation (mm)				
- Mean annual	150	231	484	643
Temperature (°C)				
- Mean high	24.6	27.5	17.1	13.4
- Mean Low	8.9	13.9	0.1	-0.7

Note: Precipitation and temperature values are from Sellers and others, 1985.

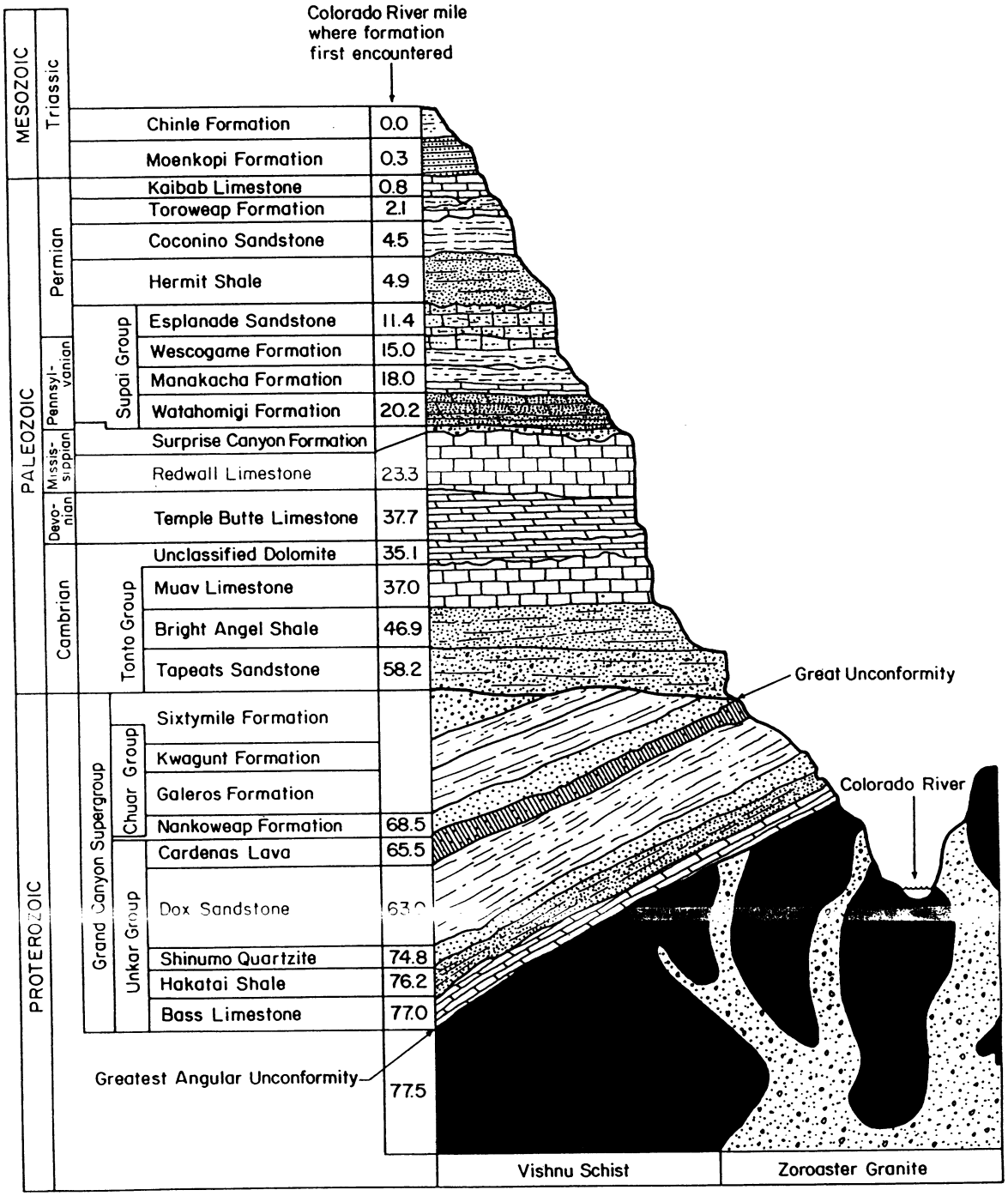

Figure 3. Stratigraphic column showing rocks exposed in Grand Canyon and the distances in river miles downstream from Lees Ferry where they first appear along the Colorado River. From Billingsley and Elston (1989).

tributaries to the Colorado River in Grand Canyon from Lees Ferry to Diamond Creek, excluding the four largest tributaries (the Paria and Little Colorado Rivers, and Kanab and Havasu Creeks). They selected those tributaries that have the potential to produce debris flows which would affect the geomorphology of the river channel. Criteria used include: 1) drainage areas larger than 0.1 km^2; 2) mapped perennial or ephemeral streams; 3) previously designated official name; 4) clear termination at the Colorado River in a single channel; 5) formation of obvious debris fans and (or) rapids.

Initiation of Debris Flows

Debris flows in Grand Canyon are initiated by a combination of intense precipitation and subsequent slope failure. The intensity of rainfall necessary to initiate debris flows in Grand Canyon is unknown, because no rain gages are located in the headwaters of debris-flow producing tributaries, but it has been estimated to be over 25 mm/hr with a total rainfall of 16 to 50 mm minimum (Webb and others, 1989; Melis and others, 1994; Table 2). The recurrence interval of precipitation levels that have produced debris flows in Grand Canyon range from less than one year to more than sixty years (Table 2). Heavy precipitation derives from three main sources in the southwestern United States: localized convective thunderstorms in summer, regional frontal systems in winter, and dissipating tropical cyclones in late summer and early fall (Hansen and Shwarz, 1981; Hirschboeck, 1985; Webb and Betancourt, 1992). Most debris flows in Grand Canyon are associated with the intense precipitation of convective summer thunderstorms that affect only one or two drainages at a time. These storms are fed by large quantities of moisture, evaporated from the northern Pacific and Gulf of California by monsoonal circulation patterns. Debris flows also occur during prolonged precipitation produced in winter by regional frontal systems. These wide-spread storms sweep across the Colorado Plateau from the west along the Pacific storm track, which is shifted south during the winter by the Aleutian Low-Pressure cell in the North Pacific. Rain that can be both widespread and intense is produced by occasional dissipating tropical cyclones in the late summer and early fall (Smith, 1986). These storms originate over the Pacific Ocean off the coast of Mexico, but occasionally travel inland when their typically north-west course is deflected to the east by low-pressure or cutoff low-pressure cells over the Pacific

TABLE 2. PRECIPITATION LEVELS DURING SOME HISTORIC DEBRIS FLOWS IN GRAND CANYON

Tributary	Location (mile-side)	Basin Area (km^2)	Date of Event (m/d/yr)	Nearest Precipitation Gage Station	Daily Precipitation (mm)	Reccurrence Interval* (yr)	Storm† Precipitation (mm)	Reccurrence Interval* (yr)
Badger Canyon	7.9-R	47.0	8/18/94	Lees Ferry	45	46	45	16
18-Mile Wash	18.0-L	5.1	8/24/87	Desert View	14	<1	17	<1
Unnamed	19.9-L	3.8	8/24/87	Desert View	14	<1	17	<1
Unnamed	62.5-R	0.7	9/18/90	Desert View	19	<1	61	34
Crash Canyon	62.6-R	1.8	9/18/90	Desert View	19	<1	61	34
Unnamed	63.4-R	0.7	9/18/90	Desert View	19	<1	61	34
Lava Canyon	65.5-L	54.7	12/5/66	Grand Canyon	43	16	118	157
Tanner Canyon	68.5-L	19.3	8/22/93	Desert View	28	3	56	8
Cardenas Creek	70.9-L	3.9	8/22/93	Desert View	28	3	56	8
Unnamed	71.2-R	1.1	8/21/84	Grand Canyon	35	3.2	69	7.6
Unnamed	72.1-R	1.2	8/21/84	Grand Canyon	35	3.2	69	7.6
75-Mile Creek	75.5-L	11.5	8/24/87	Desert View	14	<1	16	<1
75-Mile Creek	75.5-L	11.5	9/18/90	Desert View	19	<1	61	34
Monument	93.5-L	9.7	7/27/84	Grand Canyon	27	1	39	1
Crystal Creek	98.2-R	111.6	12/6/66	Tuweep	96	63	157	63
Forster Canyon	122.7-L	10.0	9/8/91	Grand Canyon	13	<1	18	1.9
Fossil Canyon	125.0-L	34.4	8/19/89	Grand Canyon	46	8	92	25
Unnamed	126.9-L	0.6	8/19/89	Grand Canyon	46	8	92	25
Unnamed	127.6-L	1.8	8/19/89	Grand Canyon	46	8	92	25
Unnamed	127.3-L	0.8	8/19/89	Grand Canyon	46	8	92	25
Bedrock Canyon	130.5-R	21.1	8/19/89	Grand Canyon	46	8	92	25

Unnamed	157.6-R	11.1	8/6/93	Peach Springs	20	<1	22	<1
Unnamed	160.8-R	3.4	8/6/93	Peach Springs	20	<1	22	<1
Prospect	179.4-L	257.2	9/6/39	Grand Canyon	32	7	98	158
Prospect	179.4-L	257.2	3/5/95	Tuweep	43	5	n.a.§	n.a.§
Unnamed	207.8-L	3.1	9/23/91	Peach Springs	35	3	n.a.§	n.a.§
Diamond Creek	225.8-L	716.7	7/20/84	Tuweep	53	10	90	24

* I estimated the probability of daily precipitation and storms using a modified Gringorten plotting position (U.S. Water Resources Council, 1981):

$$p = ((m - 0.44)/(n + 0.12)) * d ,$$

where p = probability of the event, m = the ranking of the event, n = the number of days in the record, and d = the number of days in the season. The recurrence interval, R (yrs), is

$$R = 1/P .$$

§ Storm is defined as consecutive days with measureable rainfall.

† One-day storm.

Northwest. In general, moisture and storm systems travel across Grand Canyon from west to east and south to north. There is also evidence of a strong orographic effect in the Plateau region, with increased rainfall falling at higher elevations (Table 1). It should be noted that, although intense or prolonged rainfall is necessary for the occurrence of a debris flow, in itself it is not sufficient. Debris-flow occurrence cannot be predicted solely on the basis of rainfall levels.

Debris flow source sediments in Grand Canyon consist of weathered and jointed bedrock, colluvial wedges, or sediment stored in or adjacent to channels. Numerous exposed Paleozoic and Proterozoic sedimentary strata, ranging from shale to sandstones and limestones, provide many types of source rock in a setting of high topographic relief (Fig. 3). Weathering and erosion are constantly at work on these strata as the canyon continues to widen (Ford and others, 1974; Webb and others, 1989; Hereford and Huntoon, 1990; Melis and others, 1994). Elevational and temperature gradients, along with a high degree of annual and inter-annual climatic variability, promote rock expansion/contraction as well as precipitation-related infiltration and frost action. All Grand Canyon drainage basins, particularly the largest ones, are influenced to some extent by regional and localized faults, folds and joints, which weaken bedrock to various degrees. Soft shale units erode quickly, and can destabilize overlying cliffs of more indurated sandstones and limestones. These processes result in rockfalls and rock avalanches that occur in all seasons, and under a wide variety of weather conditions, but are especially common during the winter due to prolonged precipitation and freezing temperatures. Larger slab failures also occur in the more indurated sandstones, especially the Coconino and Esplanade, as compressive stresses are released during erosive unloading.

Rockfalls and slab failures do not necessarily produce debris flows, but they do produce large amounts of colluvium, which is an important source of debris-flow material. This debris collects where softer units have eroded to form major benches, particularly the Hermit Shale, as well as the distinctive Tonto Platform formed by the Muav Limestone and Bright Angel Shale. Various shale units within the members of the Supai Group form smaller slopes that also collect loose debris (Fig. 4).

Other sources of loose, poorly sorted debris are shear zones in the many fault-controlled drainages present in Grand Canyon, such as 75-Mile Creek (river mile 75.5-L). This creek has formed along the strike of east-

Figure 4. Debris-flow source areas exposed in Monument Creek (river mile 93.5-L), Grand Canyon, Arizona. The Supai Group forms the dark, ledgy unit in the middle of the section. The overlying slope is Hermit Shale. The 1984 debris flow was initiated in the Hermit Shale and the lowest member of the Supai Group (Webb and others, 1988).

trending 75-Mile Fault, and drainages have formed preferentially along the highly fractured, footwall-side of the fault. Since 1959, three debris flows have been initiated exclusively in colluvium accumulated in these footwall sub-basins. Alluvial deposits, especially old debris-flow levees along the sides of tributary channels, also provide source sediments. Once initiated, debris flows in Grand Canyon often "bulk up", entraining sediments from terrace deposits and gaining volume and velocity as they head toward the river.

Melis and others (1994) identified four main mechanisms of debris-flow initiation in Grand Canyon: 1) the failure of weathered bedrock; 2) the "firehose effect" of runoff falling onto unconsolidated colluvial wedges, 3) direct failure of colluvial wedges, 4) combinations of the first three mechanisms (Fig. 5). The largest debris flows - which are few in number - begin with the failure of weathered Paleozoic shales and sandstones, most often in either the Permian Hermit Shale or Supai Group, although failures in other units also occur (Fig. 6). This type of failure is most often triggered by intense, localized rainfall from convective summer thunderstorms. One example of this process occurred in Monument Creek (river mile 93.5-L) in 1984 (Webb and others, 1988). On July 25, runoff from a thunderstorm centered over the eastern part of Monument Creek caused a slope failure in the Esplanade Sandstone. The failure became an avalanche that fell 650 m and mobilized into a debris flow upon reaching the creek channel. The debris flow traveled 4.5 km to the Colorado River where deposition of boulders significantly altered flow in Granite Rapid (Webb and others, 1988).

The largest number of debris flows in Grand Canyon are produced by the "firehose effect." In this mechanism, runoff pours over a cliff face, impacts colluvium below and forces a failure (Johnson and Rodine, 1984). This process frequently occurs in drainages that have waterfalls over the Redwall Limestone, with runoff falling on colluvium that overlies slopes of Muav Limestone and Bright Angel Shale (Fig. 7). As with bedrock failures, the firehose effect is usually triggered by small summer thunderstorms. However, large winter frontal systems are probably also likely to trigger this mechanism, especially in tributaries with large upper basins that concentrate runoff from widespread rainfall at a single pourover. The firehose effect triggered a debris flow in "Crash Canyon" (river mile 62.6-R) on or about September 18, 1990. Runoff from convective thunderstorms poured over the Redwall Limestone cliffs of

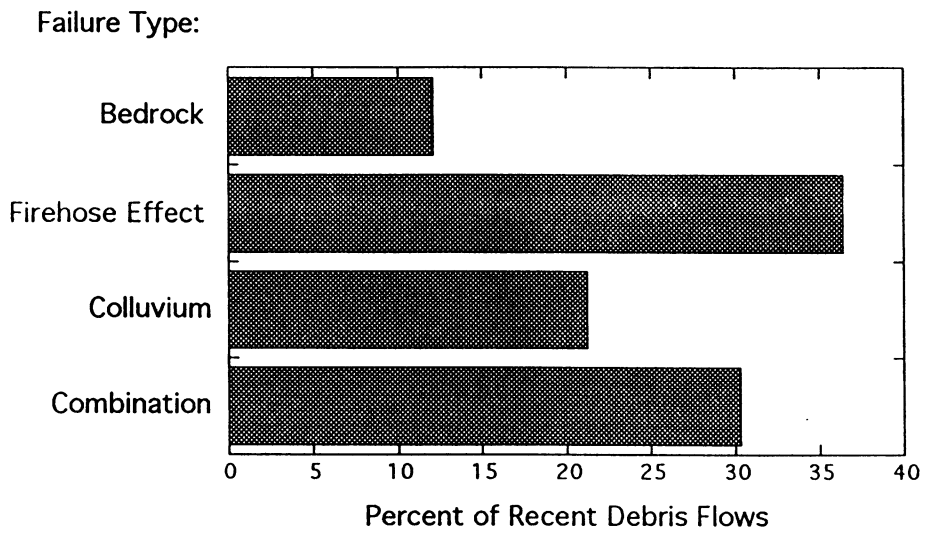

Figure 5. Percentage of each failure mechanism that has initiated debris flows in Grand Canyon between 1939 and 1994 (modified from Melis and others, 1994).

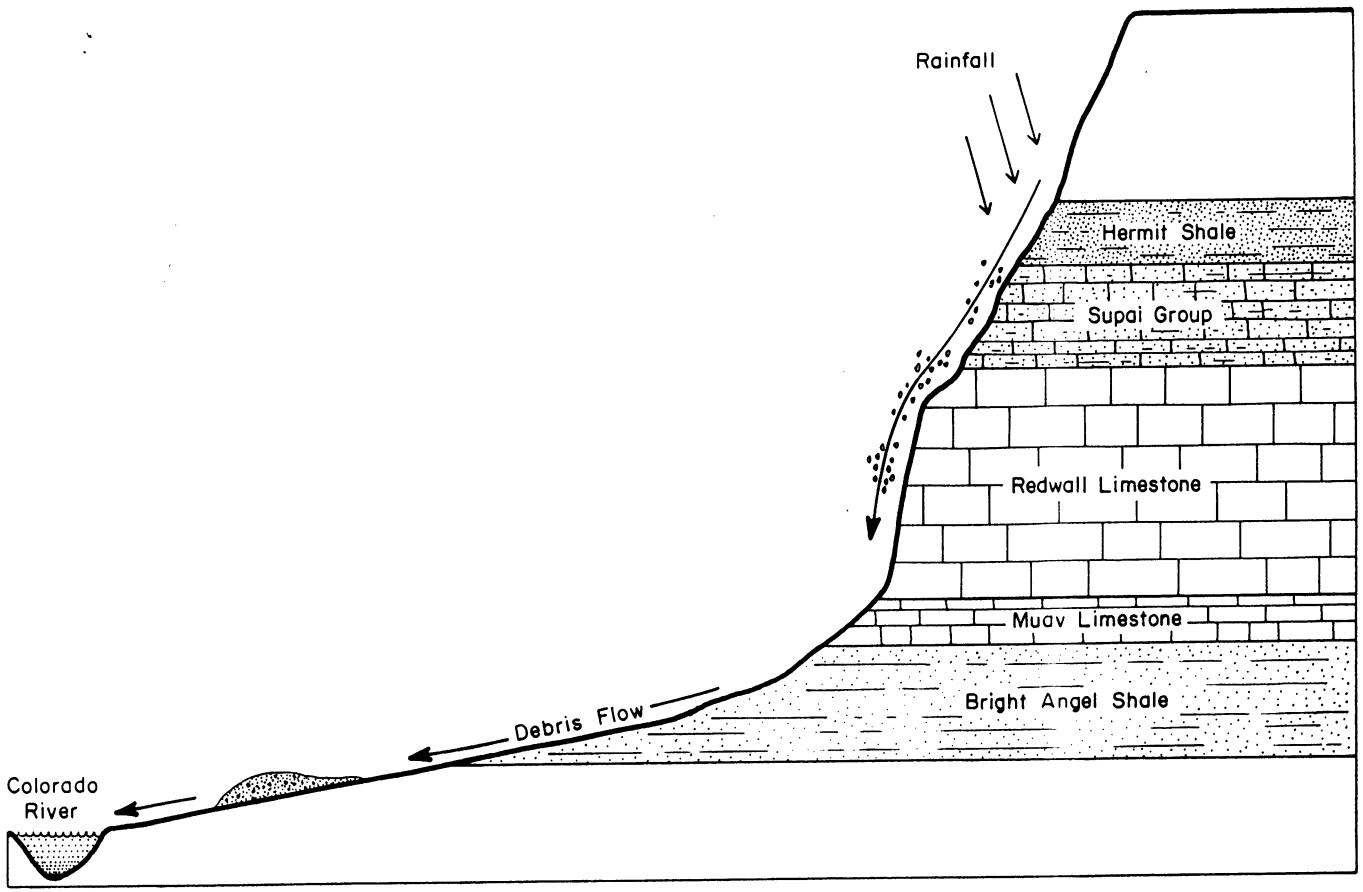

Figure 6. Schematic diagram illustrating the initiation of debris flows by the direct failure of bedrock - usually the Hermit Shale and Supai Group - during intense precipitation.

Figure 7. Failure scars caused by the "firehose effect" on colluvial wedges overlying Muav Limestone at river mile 62.5, Grand Canyon, Arizona.

Chuar Butte, falling onto massive colluvial deposits overlying Muav Limestone. The colluvium failed, resulting in a debris flow (Melis and others, 1994).

Failures of colluvial wedges occur during either intense or prolonged rainfall, and usually result in smaller debris flows (Fig. 8). In the case of low-intensity, sustained rainfall, saturation may be hastened by concentrated sheetflow runoff from cliff faces. This substantial runoff is focused at the intersection of colluvial wedge and cliff face, augmenting direct precipitation and increasing the rate of saturation. The probability of slope failure is enhanced by the lack of significant vegetation on Grand Canyon talus slopes. Multiple source areas combined with extreme topographic relief can result in combinations of the three basic initiation mechanisms.

Importance of Shale

Shales are a critical factor in the initiation of debris flows. Weathered shale bedrock fails readily, either producing debris flows directly or contributing source material to colluvial wedges. Shale units form the slopes in Grand Canyon, providing shelves upon which unconsolidated source material collects. If colluvium itself does not fail, underlying shale bedrock may, bringing overlying colluvium with it. Eroding shales also undercut more- indurated, cliff-forming lithologies, contributing to their failure. Most importantly, however, shales in Grand Canyon provide abundant fine particles and clay minerals that are essential to the mechanical stability of debris flows, giving them the internal strength necessary to transport large boulders over long distances. Grand Canyon debris flow deposits contain 1-8% silt- and clay-size particles by weight (Fig. 9). These fine particles occupy interstitial spaces in debris-flow slurries, increasing the density of the matrix and the buoyant forces that contribute to the suspension of larger particles (Beverage and Culbertson, 1964; Hampton, 1975; Rodine and Johnson, 1976). Fine-grained constituents of these debris flows are 60-80% illite and kaolinite by weight, reflecting the shales and colluvial wedges from which they originate (Table 3). Electro-chemical attraction among these clay minerals increases debris-flow matrix strength, and strong water absorption helps maintain the high pore pressures necessary to support large clasts (Hampton, 1975; Pierson and Costa, 1987).

Three lithologic units dominate the initiation of debris flows in

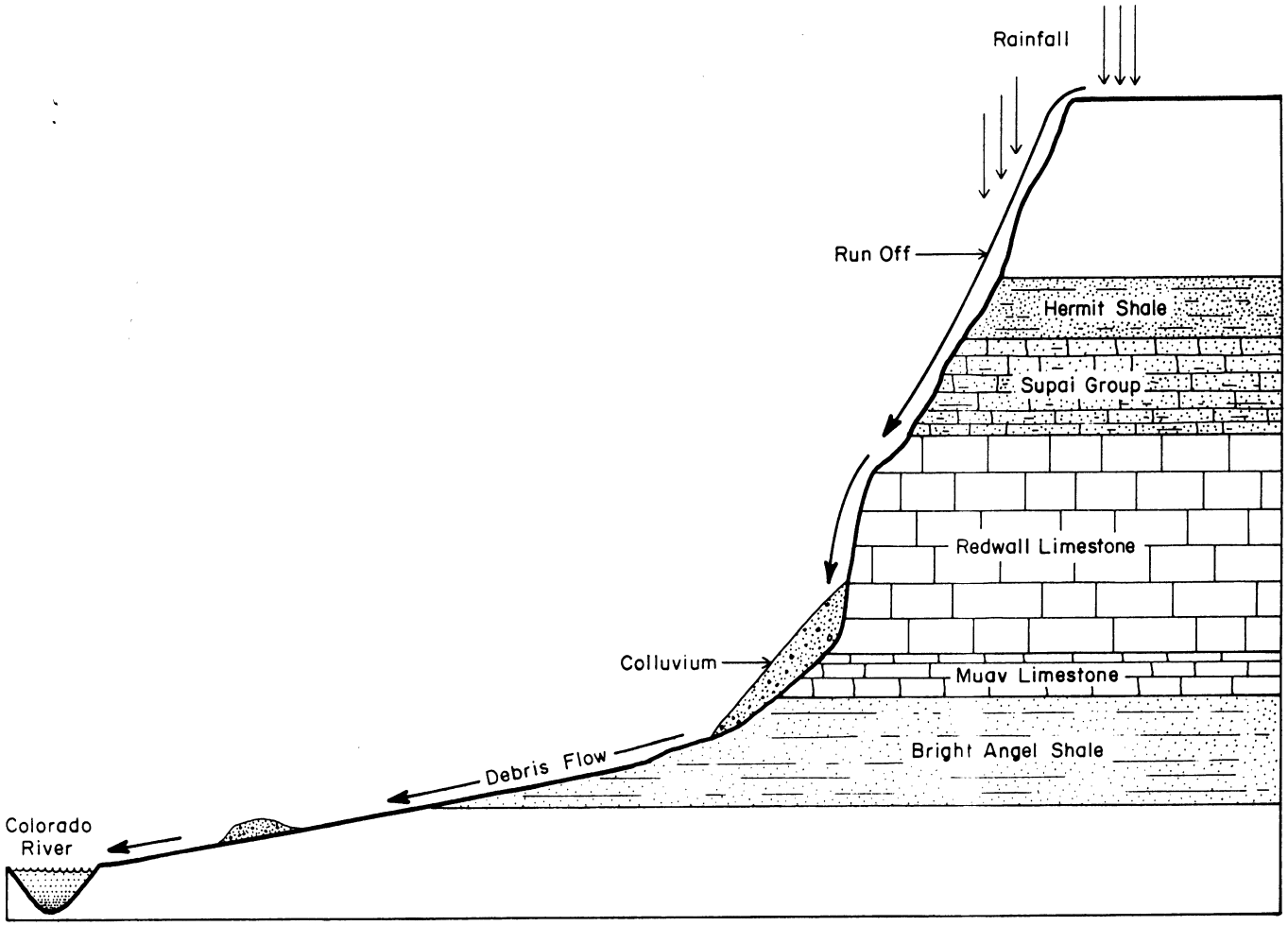

Figure 8. Schematic diagram illustrating the initiation of debris flow by colluvial wedge failure during rainfall.

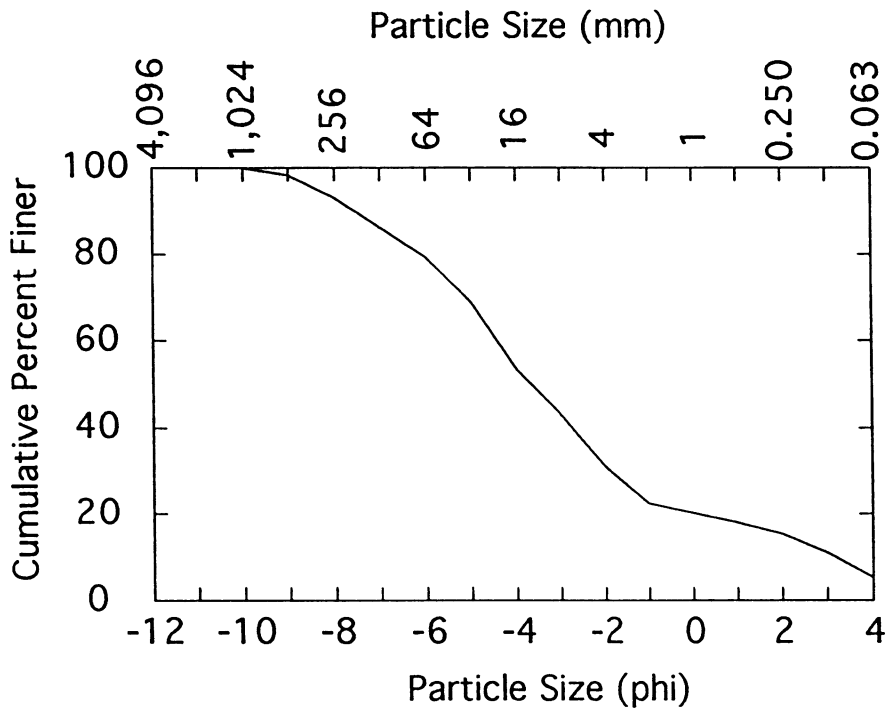

Figure 9. Particle size distribution of debris-flow deposit in "Crash Canyon" (river mile 62.6-R) during September 1990, Grand Canyon, Arizona (from Melis and others, 1994).

TABLE 3. MINERAL CONTENT OF ALL PARTICLES < .063 MM: SOURCE MATERIAL AND HISTORIC DEBRIS FLOWS IN GRAND CANYON

Sample Type	Location (mile-side)	Illite (wt %)	Kaolinite (wt %)	Smectite (wt %)	Other (wt %)
Hermit Shale	7.9-L	54	41	0	5
Esplanade Sandstone	20.5-R	50	40	2	8
Bright Angel Shale	58.0-L	68	22	0	10
Colluvium	24.4-L	29	62	0	9
Colluvium	58.0-L	20	68	0	12
Colluvium	62.2-R	32	35	7	26
Colluvium	62.5-R	43	40	8	9
Colluvium	62.6-R	22	49	2	27
Debris-flow deposit	62.6-R	58	24	0	18
Colluvium	63.3-R	49	23	10	18
Colluvium	67.2-L	10	82	0	8
Colluvium	68.5-L	22	57	0	21
Debris-flow deposit	71.2-R	19	31	0	50
Debris-flow deposit	72.0-R	48	30	0	22
Debris-flow deposit	75.5-L	62	17	0	21
Debris-flow deposit	98.2-R	42	38	0	20
Debris-flow deposit	126.9-L	43	43	2	12
Colluvium	127.3-L	44	25	17	14
Debris-flow deposit	127.5-L	38	38	0	24
Colluvium	127.6-L	45	29	6	20
Colluvium	179.4-L	35	29	6	30
Debris-flow deposit	179.4-L	34	38	4	24
Debris-flow deposit	205.5-L	56	15	8	21
Debris-flow deposit	224.5-L	60	15	6	19

Note: Mineral identification performed by semi-quantitative x-ray diffraction techniques. Margin of error ± 20% (Starkey and others, 1984).

Grand Canyon. The Hermit Shale is the most important unit of the three source areas in terms of generating debris flows. This shale is prone to both bedrock and colluvial failures, and undermines the overlying Coconino Sandstone, a source of many large boulders in eastern Grand Canyon, as it erodes. Where the Hermit Shale is first elevated to heights over 100 m above the Colorado River (about river mile 20.0), a set of some of the most closely-spaced rapids in Grand Canyon, the Roaring Twenties, begins. Although the lithology and structure of the canyon have not changed significantly at this point, the elevation of the Hermit shale beyond a threshold height above the river gives failures sufficient potential energy to transform into debris flows. Beyond this stretch of the river, the Hermit Shale is still quite influential as a source of debris flows, but has perhaps climbed too high to be contained within smaller drainages. In these cases, the lower Supai Group units or colluvial wedges of the Tonto platform may become more important in generating debris flows. The Supai Group is also a major source of bedrock failures, providing both fine particles and large boulders from interstratified shale and sandstone units. Many failures occur in the Esplanade Sandstone member, which is undercut by the erosion of a basal shale unit. The Muav Limestone, although not a shale, grades into the underlying Bright Angle Shale to form the Tonto Platform, a broad shelf at the base of the Redwall Limestone that stores abundant colluvial material throughout western Grand Canyon.

From the time of the first exploration of Grand Canyon by John Wesley Powell in 1869, the occurrence of rapids in Grand Canyon has long been linked to the presence of resistant bedrock at river level (Powell, 1875). The large boulders that form rapids are well-indurated, but they have been rafted down to the river from tributary side canyons, often over kilometers, by debris flows. The initiation of these debris flows is dependent on the presence of exposed shale units as both points of initiation and sources of fine materials. Debris flows in Grand Canyon, and ultimately the rapids they form, depend on the presence of shale source units exposed at greater than 100 m above the Colorado river. Without exposed shale units at height, rapid-forming debris flows will not occur.

Repeat Photography and Debris-Flow Frequency

Although there are a variety of possible methods for dating recent debris flows, including ^{14}C and ^{137}Cs techniques (Melis and others, 1994),

the most useful method in Grand Canyon has been repeat photography. Repeat photography has been used to identify changes in plant distribution, effects of operations of Glen Canyon Dam on sand bars, and the appearance of debris-flow and flood deposits in previous studies in Grand Canyon (Turner and Karpiscak, 1980; Stephens and Shoemaker, 1987; Webb and others, 1989; Webb, 1996). This success is due in large part to the numerous photographs that have been taken of Grand Canyon since 1872.

More than 1,159 historical photographs of the river corridor taken over the last century have been replicated and interpreted (Melis and others, 1994). Of these, 374 photographs capture views of tributary debris fans. By comparing photographs of a given debris fan taken at different times, one can identify geomorphic changes that signal the occurrence of a debris flow(s) during the time interval separating the photographs. The catastrophic nature of change in Grand Canyon means that without a debris flow, there is often little visible sign of change on debris fans, even after a hundred years (Fig. 10). In contrast, changes wrought by debris flows are usually quite obvious, including the appearance of new boulders and disappearance of old ones, extensions of debris fans, new debris levees, and/or large channels cut through old deposits (Fig. 11). For some tributaries, the dates of debris flows can be determined to within one year. However, even in these cases it is impossible to determine whether changes were the result of a single or multiple events. Thus, instead of an absolute frequency record of debris flows, a binomial frequency count was determined for each debris fan: either a debris flow(s) has occurred or not occurred over the last century.

The time interval chosen as the frequency window is just over 100 years long. This interval is determined by a remarkable baseline database of 445 photographs of the river corridor in Grand Canyon taken by Franklin A. Nims and Robert Brewster Stanton between 1889 and 1890 (Melis and others, 1994; Webb, 1996). During a survey expedition, these photographs were taken at roughly 2-km intervals along the entire length of Grand Canyon, recording the general topography of the river corridor. Added to this collection are 31 photographs of the Canyon taken by John K. Hillers in 1872 (Fowler, 1989). A total of 143 of these photographs capture debris fans at the mouths of 139 of the 529 tributaries in Grand Canyon. An additional ten tributaries were included on the basis of other photographic evidence that a debris flow reached the river at some time

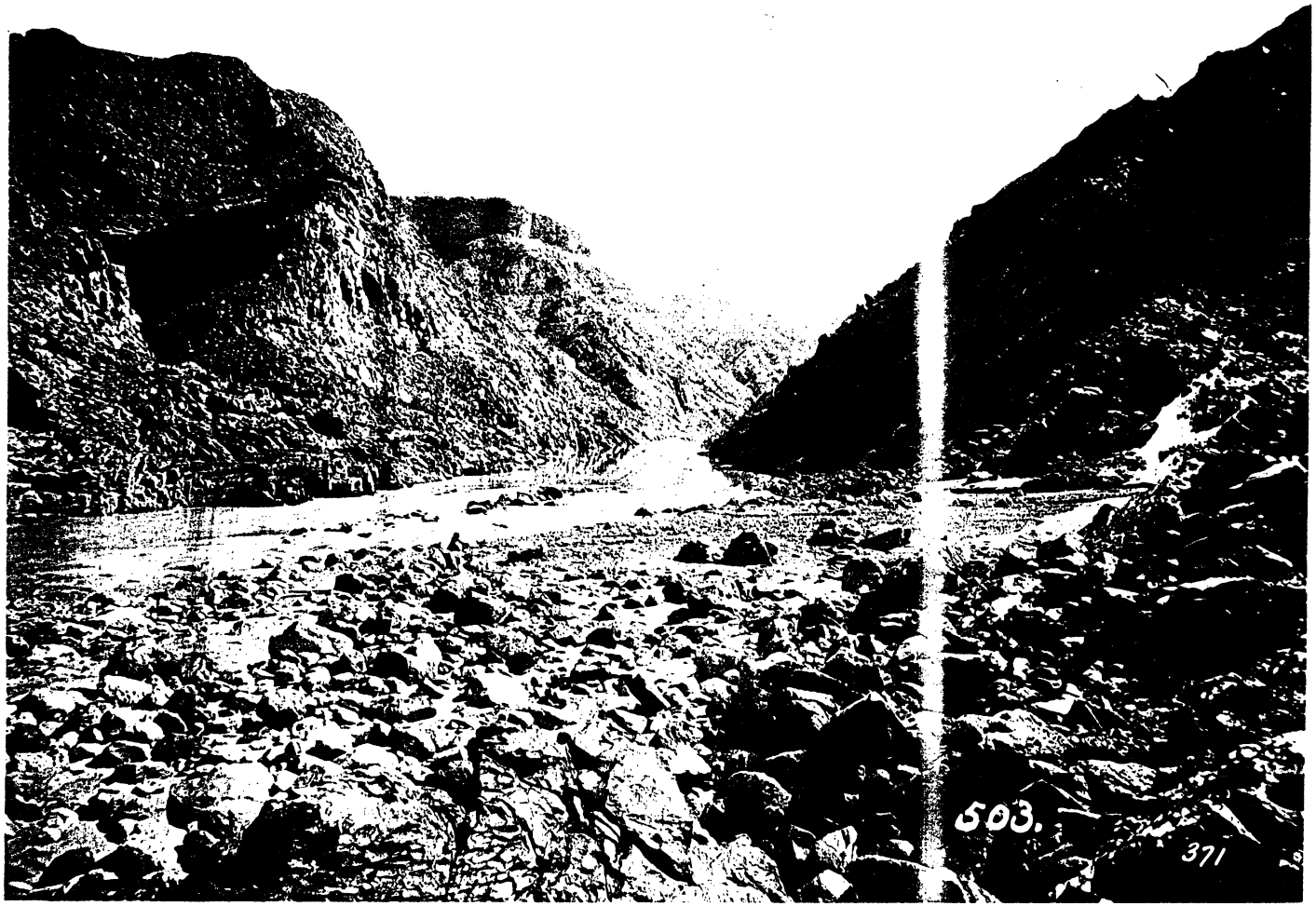

Figure 10. Matched pair of photographs taken one hundred years apart, looking across the debris fan at Ruby Canyon (river mile 104.8-L) toward Ruby Rapid (from Webb, 1996):
(A) Photograph taken on February 15, 1890 at 1:00 PM by Robert B. Stanton. Lack of sand in the canyon mouth, and fresh-looking gravels all the way to the river, indicates a flash flood had recently occurred in Ruby Canyon, probably in the summer of 1889;

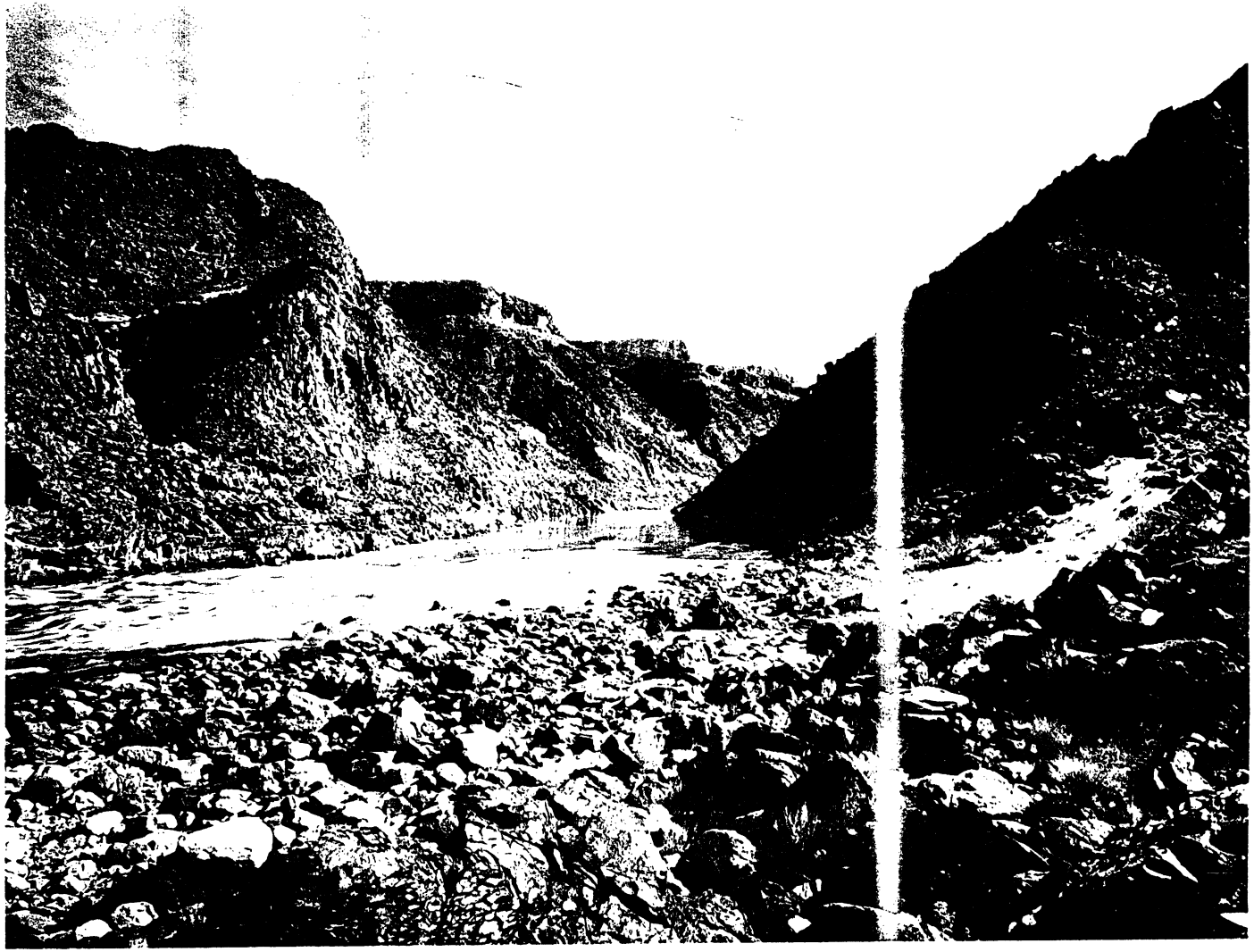

Figure 10. Matched pair of photographs taken one hundred years apart, looking across the debris fan at Ruby Canyon (river mile 104.8-L) toward Ruby Rapid (from Webb, 1996):

(B) Replicate view taken on February 14, 1991 at 2:11 PM by Ted Melis. Despite high water in 1991, the rapid and debris fan are unchanged after a century. Erosion and deposition by the Colorado River have caused the only changes in the debris fan. Instead of fresh-looking gravels at the mouth of the canyon, cobbles and boulders are now exposed. A large sand bar has been deposited at right center, obscuring a clear view of the channel mouth.

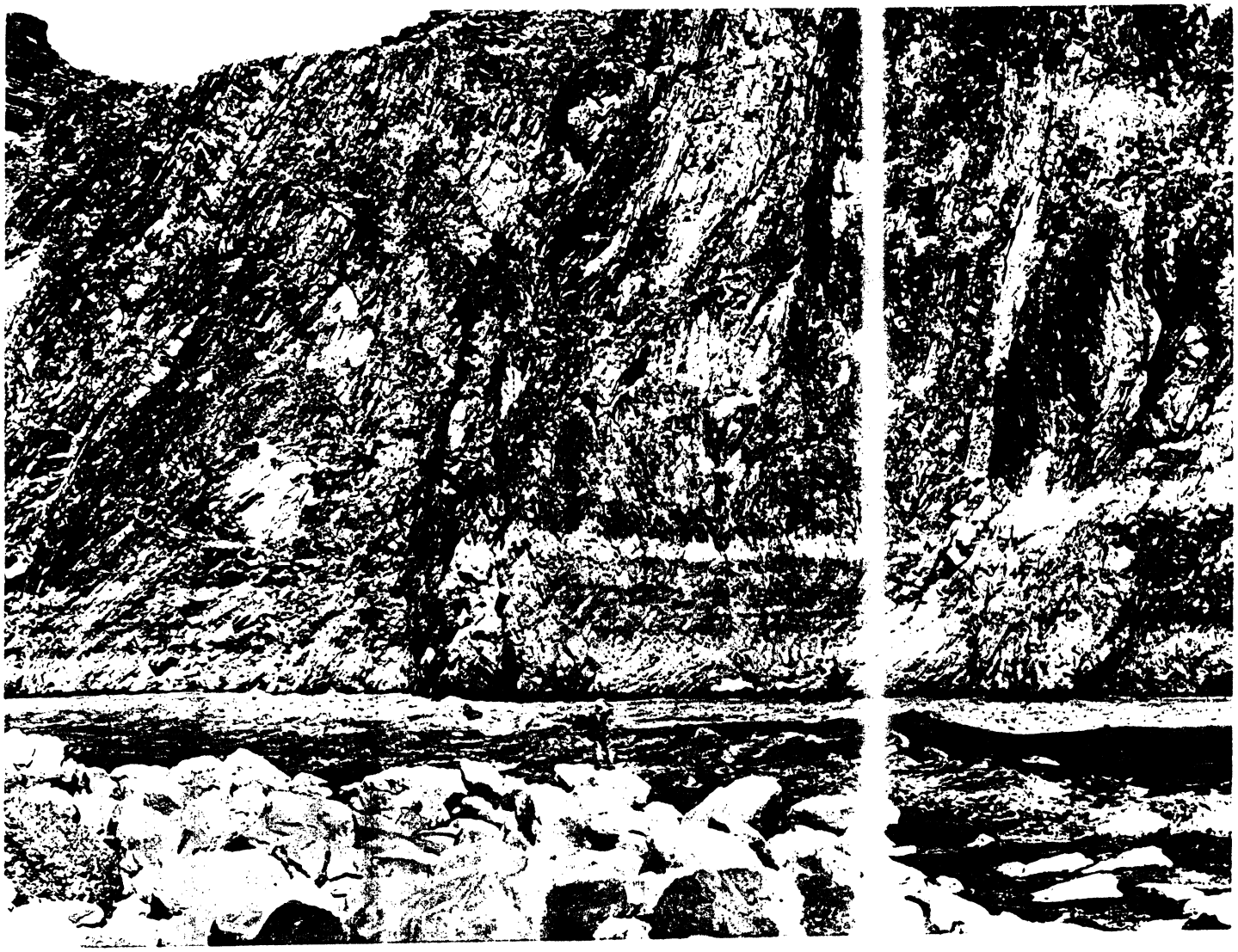

Figure 11. Matched pair of photographs looking across the debris fan at Specter Chasm (river mile 129.0-L) toward Specter Rapid (from Melis and others, 1994):
(A) Photograph taken by Clyde Eddy in 1927. Fan has been well reworked leaving only boulders exposed;

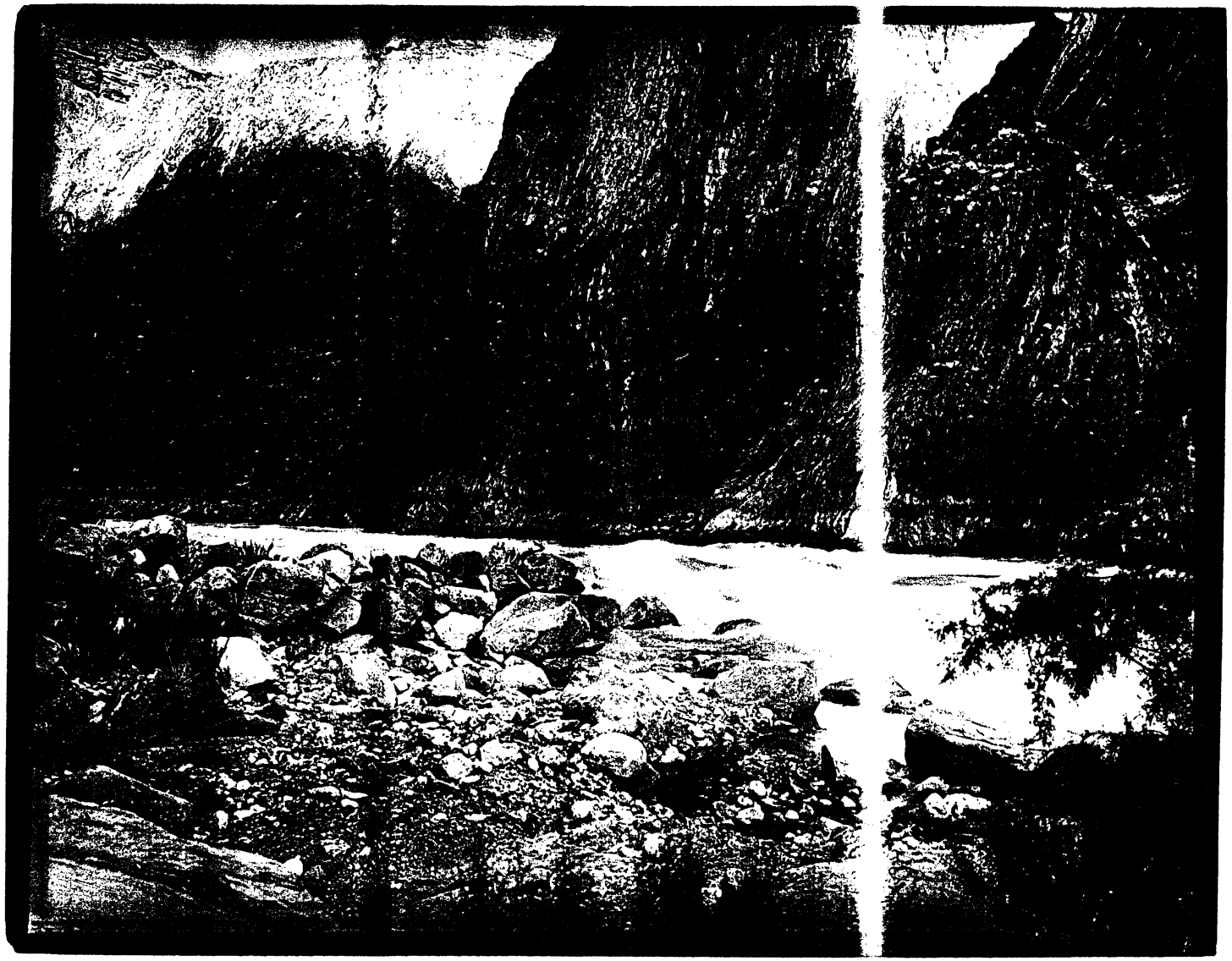

Figure 11. Matched pair of photographs looking across the debris fan at Specter Chasm (river mile 129.0-L) toward Specter Rapid (from Melis and others, 1994):
(B) Replicate view taken in 1993 by Ted Melis. A 1989 debris flow has aggraded fan with large boulders.

during the last century.

Altogether, the 149 tributary drainages represented in these photographs provide a calibration data set that was used to model the relation between debris-flow frequency and various drainage-basin parameters. The model results permit an evaluation of the importance of various field observations regarding debris-flow initiation in Grand Canyon. Frequency data were also derived from 48 additional drainages by a variety of non-photographic methods, including radiometric dating, stratigraphic evidence, and other field evidence. By combining these additional data with the calibration data, a validation data set was established in order to test the results obtained from the original, calibration data.

An important consideration in regard to the calibration data is that the photographic record examines only the mouths of tributary side canyons. Thus, frequency estimates are skewed to record only those debris flows that reached the river. Any debris flow, regardless of size, that may have flowed in a side canyon but never reached the river, is not included. Nevertheless, the photographic record of debris fans in Grand Canyon is suitably random, and the assumption is made that the 149 drainages in the calibration data set are a sufficient representative sample of the total population of 529 tributaries in Grand and Marble Canyons. The additional drainages in the validation data set were hand selected based on the best non-photographic evidence available, and therefore are not a true random sample. Nonetheless, combined with the calibration data, these data are very helpful in analyzing model results.

Morphometric, Lithologic, and Climatic Variables

Twenty variables were defined to represent various morphometric, lithologic, climatic and structural drainage basin parameters that may control or influence debris-flow initiation in Grand Canyon (Table 4). Three sets of variables relate to the potential energy of source failures and how that energy is expended in a debris flow: height above river, channel distance from river, and channel gradient. The height of source lithologies above the river represents the potential energy of failures; the higher the source, the greater the energy a failure transmits to a subsequent debris flow. The height of drainage-basin headwaters above river level does not relate directly to source failures, but to the potential energy of runoff generated during rainfall, which is itself a major factor

TABLE 4. LOGISTIC REGRESSION VARIABLES

Variable Name	Approximate Probability Distribution	Range in Values	Units
Height of Hermit Shale above river	bimodal	0-1488	m
Height of Supai Group above river	bimodal	0-1134	m
Height of Muav Limestone above river	bimodal	0-890	m
Height of head waters above river	normal	402-2207	m
Channel length from river to Hermit Shale	bimodal	0-19.8	km
Channel length from river to Supai Group	bimodal	0-15.6	km
Channel length from river to Muav Limestone	bimodal	0-10	km
Log of channel length from river to headwaters	normal	-0.3-1.8	km
Channel gradient to Hermit Shale from river	lognormal	0-2.0	none
Channel gradient to Supai Group from river	lognormal	0-0.98	none
Channel gradient to Muav Limestone from river	bimodal	0-0.64	none
Channel gradient to headwaters	lognormal	0.02-1.46	none
Elevation of Hermit Shale	bimodal	0-2073	m
Elevation of Supai Group	bimodal	0-1951	m
Elevation of Muav Limestone	bimodal	0-1707	m
Elevation of drainage-basin headwaters	normal	1061-2804	m
Southwest aspect of tributaries	uniform	0.01-0.99	none
Southwest aspect of river at confluence	uniform	0.02-0.98	none
Log of drainage basin area	normal	-1.3 - 3.0	km^2
Log of the total length of surface faults	uniform	0-193	km

in the initiation of some types of failures. High initial potential energy, however, may not translate into a rapid debris flow if there is a long transit distance to the river. Therefore, the channel distance to source lithologies and drainage headwaters was also measured. The greater this distance, the more energy is lost in transport, and fewer small debris flows reach the river. These competing variables are combined in a third variable measuring channel gradient to source lithologies and drainage headwaters. Drainages with steep gradients (source vertically far above and laterally close to the river) represent high-energy environments where source failures are more likely to both transform into debris flows and reach the river.

The interrelation of these three variable types makes it unlikely that there is a simple linear relation between each variable and debris-flow frequency. For each case, debris-flow frequency likely increases rapidly to an optimum, then decreases. As source area rises, channel distance increases, and energy dissipation eventually begins to outweigh increases in potential energy. Alternately, as source areas approach the river, channel distances decrease, but so does height above river, and there is little potential energy to initiate debris flows. Similarly, the steepest, high-energy gradients occur in the smallest drainages where source areas are not always sufficiently high above the river to generate debris flows.

The lack of suitable precipitation data necessitated the derivation of various proxy variables for climatic effects. Elevation of source lithologies and basin headwaters above sea level is included to reflect orographic effects on precipitation. Higher elevations are likely to intercept more moisture as precipitation and so produce more debris flows. Additionally, tributaries which open into the path of weather systems and moisture vectors may actively trap precipitation, particularly smaller storms. Thus, an aspect measure for each drainage was measured as the angle from true north of a ray drawn from the basin centroid to its confluence with the river. This radial measure was then transformed into a linear value more appropriate for logistic regression modeling: southwestern aspect. This variable represents the degree to which a given drainage faces southwest (southwest = 1.0, northeast = 0.0, southeast/northwest = 0.5, etc.). A southwest orientation was chosen to reflect the southwest to northeast travel vectors of severe weather across the canyon. Similarly, the aspect of the canyon or river-corridor

itself likely controls whether moisture will travel into drainage basins or not. Moisture is likely to pass over the canyon where it moves perpendicular to the river, especially where the canyon is narrow (eastern Grand Canyon). In contrast, where the river parallels the storm track, there is the possibility of moisture moving down into the canyon and being trapped within tributary drainages. Therefore, river aspect was measured as the angle from true north of a vector drawn parallel to the river in its direction of flow at the confluence of each tributary. This value was then linearized into a variable measuring how southwest/northeast (1.0) to northwest/southeast (0.0) the river corridor runs.

Drainage-basin area also relates to debris-flow frequency. Larger drainages generally provide more source material and are more likely to be hit by localized thunderstorms (a simple increase in probability with target area). They also produce more runoff during widespread precipitation, especially those basins with large drainage areas above the canyon rim, such as Prospect Creek (river mile 179.4-L). As with other variables, however, the relation between drainage area and debris-flow frequency is not linear. Source material increases with drainage area to a certain point, after which source areas simply retreat from the river with the cliff face in a linear fashion without an increase in exposed area. Also, larger drainages have shallower gradients and longer channel distances, making it less likely that debris flows will reach the river. As with other non-linear parameters, there may be an optimum drainage size above which debris-flow frequency begins to decrease.

The influence of geologic structure in each drainage was evaluated as the sum of all surface faults delineated on geologic maps of the Grand Canyon area (Haynes and Hackman, 1978; Huntoon and others, 1981; Huntoon and Billingsley, 1983; Huntoon and others, 1986). One important difficulty with this data is that geologic map coverage of the study area is not at a uniform scale: map scales ranged from 1:250,000 to 1:48,000. Thus, on the basis of scale variation alone, apparent fault density may differ from one area to another depending on the map used. In this case, density may increase artificially from east to west, because map scales increased in that direction.

All drainage-basin parameter data were derived from USGS 7.5' topographic maps and various geologic maps (Haynes and Hackman, 1978; Huntoon and others, 1981; Huntoon and Billingsley, 1983; Huntoon and others, 1986). For source lithologies, elevations, heights above and

channel distance from the river were averaged between the greatest and smallest value measured to the bottom of the unit. For lithologic strata that are not present in a given basin, zero values were entered for their related parameters. Gradient was calculated simply as height above river divided by channel distance, and so is also a mean value. Drainage-basin boundaries were drawn by hand on topographic maps, and digitized into a MIPS GIS, which calculated basin areas and centroids.

In order to take into account the spatial variability evident in these basin variables across the 9516 km^2 study area, three calibration data sets were extracted from the variable data. The first set represents all 149 drainages for which there is frequency data. This set is used to develop a general model relating drainage-basin parameters and debris-flow frequency for the entire canyon. This data set was also split in half, with 75 drainages comprising a data set representative of eastern Grand Canyon (largely Marble Canyon) and 74 drainages representing western Grand Canyon. This division falls at river mile 95.0, where the Colorado River bends to the northwest. This point is reasonably close to Phantom Ranch (river mile 87.8), a traditional point of division between eastern and western Grand Canyon. These two reduced data sets were used to develop separate models for eastern and western Grand Canyon. The validation data set was divided in the same way.

Logistic Regression

Because the dependent variable, debris flow frequency, is binomial, logistic regression was chosen to model the relation of drainage-basin variables to debris-flow frequency. Where linear regression returns a continuous value for the dependent variable, logistic regression returns the probability of a positive binomial outcome (in this case, debris-flow occurrence during the last century). Logistic regression is commonly used in medical and biological studies where the dependent variable is the presence or absence of a given illness or disease, and independent variables the presumed controlling factors. Logistic regression can then be used to analyze the statistical significance of certain factors in relation to the disease, as well as for modeling the probability of contracting the disease on the basis of the significant controlling factors (Hosmer and Lemeshow, 1989).

For logistic regression, the conditional mean ($\pi(\mathbf{x})$) is :

$$(\pi(\mathbf{x})) = e^{g(\mathbf{x})} / [1 + e^{g(\mathbf{x})}]$$

where:

$$g(\mathbf{x}) = \beta_0 + \beta_1 x_1 + \beta_2 x_2 + \ldots + \beta_i x_i \qquad (i = \text{number of variables})$$

Variable parameter coefficients (β_v) are estimated by the method of maximum likelihood, where those coefficients with the highest probability of returning the observed values are selected. Maximum likelihood is determined using the likelihood function, which expresses the probability of the observed data as a function of the unknown coefficients (Hosmer and Lemeshow, 1989). Those coefficients that maximize the likelihood function are thus the coefficients with the greatest probability of returning the observed values. SAS statistical software was used to calculate these model coefficients as well as various measures of their significance (SAS, 1990).

Several of the measures of statistical significance in logistic regression modeling are derived from the likelihood ratio test. This test compares two models:

$$\mathbf{G} = -2 \ln [\text{ likelihood of model B / likelihood of model A }]$$

where model B is composed of a subset of the variables in model A. Under the hypothesis that the coefficients of the variables not contained in B are equal to zero (that is, that these variables contribute nothing to model A, which is then no different than model B, and $\mathbf{G} = 0$), the statistic G will follow a χ^2 distribution with degrees of freedom equal to the number of variables not present in B. A χ^2-based probability value (ρ) can then be determined from **G** with the null hypothesis that there is no difference between the models. If ρ is sufficiently small, the null hypothesis is rejected and model B is significantly different from model A.

Using the χ^2-based probability values, the significance of individual variables within a model can be evaluated. In this case, model A contains the variable in question, model B does not, and the probability value obtained (ρ_v) measures the significance of the variable, the only difference between models A and B. In order to obtain the optimum model - that is, a model with the fewest possible variables that still effectively explain the observed data - I used a step-backward elimination procedure. In this technique, an initial model is calculated with parameter coefficients and significance probabilities estimated for each variable. The variable with the least significance (highest ρ_v) is then eliminated from consideration and a second model is calculated without that variable.

This process continues, eliminating an additional variable at each step until the only variables that remain have a significance probability less than a given threshold. Only those variables with $\rho_v < 0.05$ remain in the model. Those variables which do not significantly contribute to the model in statistical terms have been eliminated.

The significance of the eliminated variables as a group can be evaluated by measuring the probability (ρ_m) that the current model is significantly different from the initial, twenty-one variable model. If $\rho_m > 0.05$, the current model is not significantly different from the initial model, thus the eliminated variables as a group were not significant. This statistic can also be used to evaluate how easily significant variables are differentiated from non-significant variables, or rather, how clear cut the model is. If ρ_m approaches 1, then significant variables were easily differentiated from non-significant variables, and little explanatory power was lost in removing non-significant variables. As ρ_v approaches 0.05, however, the distinction between significant and non-significant variables was more difficult to determine, and more explanatory power, even if not statistically significant, is lost with the removal of non-significant variables. This provides one simple measure of model robustness.

In order to further test robustness, models were derived from the validation data sets and compared with the calibration models. The more closely the validation models replicated the calibration models, the more representative the calibration models are likely to be of the areas of Grand Canyon concerned. There are some problems inherent in using calibration data in the validation data set (75% of the validation data is calibration data), but the number of drainages with frequency data is limited. Trends indicated by model comparison are nonetheless useful.

A rough measure of model accuracy (α) was also calculated. This value is a percentage of how often model predictions match observed data. Binomial frequency values are obtained by rounding off predicted probability values to whole numbers. Finally, in addition to calculating multivariate models using all twenty-one basin variables, univariate models of the relation between debris-flow frequency and each basin variable individually were calculated. These univariate model results reveal which variables attain significance only in combination with other variables.

Logistic regression is essentially a linear method. Therefore, an attempt was made to identify and correct for non-linear relations between basin variables and debris-flow frequency during the modeling process. Following methods outlined in Hosmer and Lemeshow (1989), suspect variables were identified by examining the plot of the variable value against g(**x**) for non-linear trends. These variations were accounted for by adding appropriate additional variables (such as the square of the given variable for parabolic trends) to the model. None of the corrections for nonlinearity altered the final model results. Therefore, the assumption was made that the relation between debris-flow frequency and drainage-basin parameters can be effectively described using a linear model. Each significant variable was also ranked within each final model by calculating a standardized coefficient for each. The logistic regression procedure in SAS statistical software provides a standardized coefficient derived by multiplying the coefficient by the ratio of the standard deviation of the underlying distribution to the sample standard deviation of the variable. When evaluated, however, these standardized coefficients were extremely unstable between calibration and validation models. Therefore, standardized coefficients were dropped as a method of ranking variable importance.

Analysis

In modeling debris-flow frequency for all of Grand Canyon (river mile 0 to 225.8), stepwise elimination removed fifteen of the initial twenty drainage-basin variables as not statistically significant (Table 5). For the final, five-variable model, $\rho_m = 0.89$, indicating that the model is not significantly different from the initial, twenty-one variable model, and that little explanatory power has been lost. The model is therefore well defined and reasonably accurate, correctly matching 70% or greater of the observed frequencies. The validation model produces the same significant variables (Table 5), as well as four new variables. These new variables were among the last five eliminated from the calibration model. The validation model was generated with $\rho_m = 0.74$, indicating that the larger data set was more difficult to differentiate on the basis of significant and non-significant variables. Nevertheless, the final model was not significantly different from the initial model. Channel gradient to basin headwaters was not significant in the validation model, but it was the last non-significant variable to be eliminated.

TABLE 5. GENERAL DEBRIS-FLOW FREQUENCY MODEL FOR GRAND CANYON, ARIZONA

Independent Variable	Coefficient	Significance		Accuracy
		Variable	Model	
	(β_v)	(ρ_v)	(ρ_m)	(α)
Calibration Model:				
- Intercept	-0.9133	0.4104	0.89	0.70
- Height of headwaters above river	-0.0024	0.0048		
- Log of drainage-basin area	2.0398	0.0076		
- Channel gradient to headwaters	5.4632	0.0328		
- Aspect of river	1.4866	0.0346		
- Channel gradient to Hermit Shale	2.1655	0.0380		
Validation model:				
- Intercept	0.2846	0.7257	0.77	0.72
- Channel gradient to Hermit Shale	6.6689	0.0004		
- Channel distance to Muav Limestone	0.7731	0.0012		
- Elevation of Hermit Shale	-0.0016	0.0026		
- Channel gradient to Muav Limestone	4.8826	0.0078		
- Log of drainage-basin area	1.2020	0.0087		
- Height of headwaters above river	-0.0020	0.0219		
- Aspect of river	1.6612	0.0346		
- Height of Muav Limestone	-0.0038	0.0456		

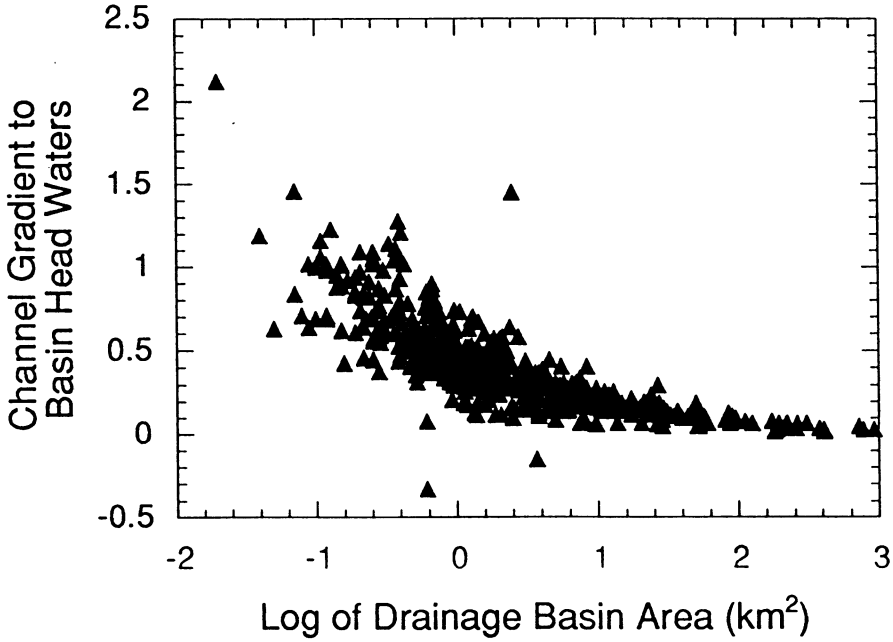

Figure 12. Plot of the inverse relation between drainage-basin area and gradient for 529 tributaries in Grand Canyon, Arizona.

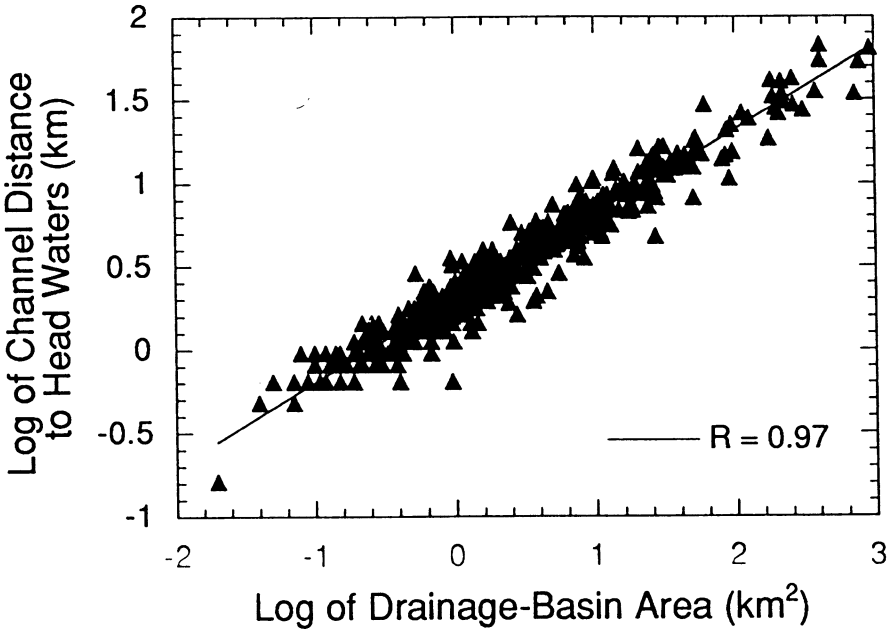

Figure 13. Plot of the linear relation between drainage-basin area and the total channel length from head waters to river confluence for 529 tributaries in Grand Canyon, Arizona. Linear regression resulted in R=0.97.

Three types of variables are represented in the general model: general morphometric variables, lithologic variables, and climatic variables. The general basin morphometric variables are the log of drainage-basin area, channel gradient to head waters, and height of basin head waters above the river. Both basin area and channel gradient are positively related to debris-flow frequency: large drainages and steep gradients produce more debris flows. The linking of debris-flow production to the maximization of two variables that are inversely proportional to each other (Fig. 12) helps to illustrate the complexity of the initiation process. The height of drainage-basin head waters above river level is negatively related to debris-flow frequency: more debris flows are produced in drainages where the head waters are vertically close to the river. This result is the opposite of what was expected if this variable reflects the potential energy of basin runoff. However, most basin head waters are quite high already (mean value is 1200 m above the river), and potential energy may already be optimal, and not much of a differentiating factor. This variable is more likely to be acting as an indirect measure of travel distance, which does become more important as it increases. Basins where the headwaters are laterally close to the river tend to produce more debris flows. The measure of channel distance to basin head waters itself is demonstrably an effective measure of basin size (linear correlation with drainage area: R=0.98; Fig. 13), and may not be as effective a measure of travel distance as height above head waters. It may be that none of the channel distance measures are adequate measures of debris-flow travel distance.

The only lithologic variable retained in the general calibration model is the average channel gradient from the Hermit Shale to the river. This indicates that of the three source areas considered -- the Hermit Shale, Supai Group, and Muav Limestone -- the Hermit Shale is the most consistently influential in producing debris flows throughout the canyon. The selection of a gradient variable confirms that both vertical height above and lateral closeness to the river play important roles in determining the productivity of this shale source area in generating debris flows. Although the Hermit Shale is the highest of the three source areas, it is not as high as basin headwaters (mean value of 800 m above river level), so potential energy increases with source height are still a factor in debris flow production. The importance of source areas in general is

amplified in the validation results, where all four of the additional variables are lithologic in nature. The validation model also suggests that the Muav Limestone is the second most influential source area in producing debris flows.

The least influential, but significant, variable is the aspect of the river corridor at the tributary confluence, which is a proxy for climatic effects. River aspect is positively correlated with debris-flow frequency, indicating that more debris flows occur in tributaries where the river corridor trends northeast/southwest, parallel to the general movement of severe weather across Grand Canyon. Fewer debris flows occur where the river trends northwest/southeast, perpendicular to storm movement. Although tributary aspect was not selected as significant, it is somewhat reflected in the river aspect variable as 80% of tributary aspects lie between 45° and 135° to the local river aspect. Thus, tributaries with a generally western aspect would likely be most influenced by weather coming up the canyon. Clearly, however, river aspect is the controlling factor, as indicated by its selection in the models.

The remaining climatic variables, all elevation measures, were not included in the calibration model. It may be that orographic effects due to variation in elevation are not strong enough to affect debris-flow production differently in different drainages. Thus, although of importance locally, simple orographic effects form more of a general background signal that is not useful in statistically distinguishing drainages on the basis of debris-flow production. This may also be the reason for the absence of degree of tributary faulting from the general model. Arguably, although the location of many tributaries is controlled by the location of major faults (Dolan and others, 1978), the influence of tributary faulting on debris-flow production is difficult to quantify, and this particular variable may not be a sufficient measure of its influence. Nevertheless, faulting has at best an indirect impact on debris flows. It is ubiquitous in the canyon, especially in the west, and may not vary consistently enough from one drainage to another to influence debris-flow production noticeably in the general case.

Overall, the collection of variables retained in the general model reflects the complexity of the initiation process. As noted, some variables work at odds with each other, such as steep gradients and large drainage-basin areas, and can not be reconciled without compromise. This difficulty is rooted in the interconnectedness of many of these variables:

headwaters drop and channel distances shrink with drainage area while gradient increases. In the model itself, these variables are shown to be not only inter-related, but interdependent, as illustrated by the univariate modeling results (Table 6). Only two of the five significant variables in the multivariate model were also significant when modeled singly against debris-flow frequency in univariate models: channel gradient to the Hermit Shale and river aspect. The three morphometric variables -- basin area, channel gradient to head waters, and height of head waters -- become significant only in combination with each other. Debris-flow initiation in Grand Canyon is a complex process where the variables involved not only act singly but interact dynamically to generate debris flows.

Although the general model of debris-flow frequency for Grand Canyon is reasonably clear cut and accurate, it masks a certain heterogeneity in drainage-basin characteristics throughout the canyon. The drainage area of the Colorado River in Grand Canyon that was sampled from is quite large (9516 km^2), and different geographic sub-regions within this area display distinctly different characters. At the most basic level, data for eastern Grand Canyon (river mile 0 to 95.0) can be distinguished from western Grand Canyon (river mile 95.0 to 225.8). This heterogeneity is well illustrated by the contrasting results obtained from models calculated for each data subset. In eastern Grand Canyon, fourteen variables were rejected in the modeling process to produce a final, six-variable model (Table 7). For this model, $\rho_m = 0.97$, indicating that the overall significance of the rejected variables was negligible. Essentially no explanatory power was lost in reducing the model. The result is a well-defined and fairly accurate model that correctly matches observed frequencies 77% of the time. This increase in accuracy over the general model is due in part to the increased number of variables involved, but also to the increased geologic homogeneity of a smaller sample region. The eastern model is also very robust, as four of the six variables were reproduced exactly and two replaced by similar variables in the validation model (Table 7).

Significantly, the five core variables of the eastern model exactly replicate the general model. This suggests that drainage characteristics in the east are more homogenous than in the west, allowing significant variables to be more easily isolated into a definitive eastern model that largely determines the general model. The additional variable, height of

TABLE 6. UNIVARIATE DEBRIS-FLOW FREQUENCY MODELS

Independent Variable	Variable Significance (ρ_m)		
	general model	eastern model	western model
Height of Hermit Shale above river	0.4387	0.6301	0.9858
Height of Supai Group above river	**0.0203***	0.4240	0.0931
Height of Muav Limestone above river	**0.0256***	0.4861	**0.0155***
Height of headwaters above river	0.0980	0.7200	0.2080
Channel length to Hermit Shale	0.4858	0.5005	0.8494
Channel length to Supai Group	0.2963	0.5171	0.7453
Channel length to Muav Limestone	0.1539	0.7661	0.0857
Log of channel length to headwaters	0.6029	0.9953	0.6313
Channel gradient to Hermit Shale	**0.0076***	**0.0479***	0.2475
Channel gradient to Supai Group	0.8236	0.7926	0.9065
Channel gradient to Muav Limestone	0.7784	0.2584	0.0860
Channel gradient to headwaters	0.1664	0.3123	0.4686
Elevation of Hermit Shale	0.7736	0.8233	0.9854
Elevation of Supai Group	0.1670	0.9428	0.0877
Elevation of Muav Limestone	**0.0253***	0.2611	**0.0208***
Elevation of headwaters	0.2471	0.8273	0.1338
Tributary aspect	0.8697	0.1502	0.6750
Aspect of river at confluence	**0.0006***	**0.0015***	0.1231
Log of drainage-basin area	0.7152	0.7898	0.6568
Total length of surface faults	0.8654	0.5644	0.6902

* Statistically significant values ($\rho_v < 0.05$).

TABLE 7. DEBRIS-FLOW FREQUENCY MODEL FOR EASTERN GRAND CANYON, ARIZONA

Independent Variable	Coefficient	Significance		Accuracy
		Variable	Model	
	(β_v)	(ρ_v)	(ρ_m)	(α)
Calibration Model:				
- Intercept	-4.8488	0.0214	0.97	0.77
- Log of drainage-basin area	5.4429	0.0056		
- Channel gradient	15.2610	0.0106		
- Aspect of river at confluence	3.3230	0.0183		
- Height of headwaters above river	-0.0054	0.0243		
- Height of Muav Limestone	0.0044	0.0339		
- Channel gradient to Hermit Shale	4.0361	0.0454		
Validation Model:				
- Intercept	-3.9582	0.0128	0.75	0.78
- Elevation of Hermit Shale	-0.0026	0.0016		
- Aspect of river at confluence	3.1597	0.0024		
- Channel distance to Muav Limestone	0.5999	0.0030		
- Channel gradient to Hermit Shale	7.1965	0.0043		
- Log of drainage-basin area	2.0255	0.0128		
- Channel gradient to headwaters	6.4927	0.0382		

the Muav Limestone above the river, continues the theme seen in the general validation model: Muav Limestone is the second most influential source area after the Hermit Shale. Notably, only the height of the Muav above river level is selected, not channel gradient. This is likely due to the generally low height of the Muav Limestone relative to other source areas (in eastern Grand Canyon, non-zero height values for Muav Limestone average 400 m compared with 611 m for the Hermit Shale). Travel distance to the river is so small that variation in gradient has little effect. More important is the acquisition of sufficient energy to transform failures into debris flows. Thus, those drainages that have the Muav Limestone higher produce more debris flows. Similarly, in the validation model, height to the Muav Limestone is replaced by channel distance to river. Positively related to debris-flow frequency, it has the same effect of favoring those drainages where the Muav Limestone is farther from, and thus higher above, the river. The Hermit Shale, highest of the source areas, produces the opposite effects. It rapidly gets high enough above the river that gradient and travel distance are significant factors. Thus, those drainages where the Hermit comes closer to the river produce more debris flows. These drainages tend to have higher gradients and lower elevations of Hermit Shale.

In the model for western Grand Canyon, only twelve variables were rejected to produce a final, eight-variable model (Table 8). In this case, $\rho_m = 0.39$, which again indicates that the final model is not significantly different from the initial model. The fact that ρ_m is substantially lower than in the general and eastern models, however, indicates that the discrimination of significant from non-significant variables is more difficult in the western canyon. This again reflects the comparative heterogeneity of western Grand Canyon; it is difficult to identify consistent patterns of association between drainage-basin parameters and debris-flow frequency. This model also has good accuracy ($\alpha = 0.74$), but this is most likely due to the larger number of explanatory variables.

The heterogeneity of basin parameters in the western canyon is also reflected in the volatility of the model. Only two variables remain constant between the calibration and validation models (Table 8). The model is not at all robust, and this makes evaluation of specific variables unfeasible. However, one can discern general trends that are consistent for the two models, such as the distinct lack of general morphometric and climatic variables. Instead, there is an overall emphasis on lithologic

TABLE 8. DEBRIS-FIOW FREQUENCY MODEL FOR WESTERN GRAND CANYON, ARIZONA

Independent Variable	Coefficient	Significance		Accuracy
		Variable	Model	
	(β_v)	(ρ_v)	(ρ_m)	(α)
Calibration Model:				
- Intercept	-0.9133	0.4104	0.89	0.70
- Height of headwaters above river	-0.0024	0.0048		
- Log of drainage-basin area	2.0398	0.0076		
- Channel gradient to headwaters	5.4632	0.0328		
- Aspect of river	1.4866	0.0346		
- Channel gradient to Hermit Shale	2.1655	0.0380		
Validation model:				
- Intercept	0.2846	0.7257	0.77	0.72
- Channel gradient to Hermit Shale	6.6689	0.0004		
- Channel distance to Muav Limestone	0.7731	0.0012		
- Elevation of Hermit Shale	-0.0016	0.0026		
- Channel gradient to Muav Limestone	4.8826	0.0078		
- Log of drainage-basin area	1.2020	0.0087		
- Height of headwaters above river	-0.0020	0.0219		
- Aspect of river	1.6612	0.0346		
- Height of Muav Limestone	-0.0038	0.0456		

variables. Five of the eight variables remaining in the calibration model and all five variables in the calibration model are lithologic in nature, measuring the height of a source area above the river or channel gradient to the source area. This emphasis probably reflects the chaotic nature of western Grand Canyon, due to increased faulting and the interplay of various source lithologies as they rise and fall. The only two consistent variables between models, channel gradient to Hermit Shale and Muav Limestone, are lithologic variables and indicate that the Hermit Shale and Muav Limestone continue to be the dominant source areas in this section of Grand Canyon. There is also an indication that the Supai group has an increased importance in western Grand Canyon. This may be because there are more basins in the west, where the canyon is wider, that do not reach high enough to contain the Hermit Shale. Thus, the Supai Group, the next highest source area, plays more of a role in generating debris flows.

The lack of significant morphometric variables in the western model is striking in comparison to eastern Grand Canyon. This absence does not suggest that these parameters play no role in producing debris flows in the west, simply that they do not play as great a role. Drainages in the west are on average larger, with shallower gradients and less variability in variables. Thus, morphometric measures may not be as discriminating as lithologic variables in debris flow production. The canyon is also wider in the west with mean basin channel length 1.2 km longer in the east. This may explain in part the lack of climatic variables, such as river aspect, in the western model. Moisture is more likely to move into a wider canyon, even if it lies perpendicular to the storm track. Source-area elevation variables do appear in the western models, but their negative relation to debris-flow frequency suggests that their function is related to source area placement more than orographic precipitation effects.

Conclusions

Debris flows in Grand Canyon present an important control on the Colorado River, depositing large, rapid-forming boulders that control the river's longitudinal profile. These mass movements are initiated when weathered bedrock or colluvial wedges fail during intense rainfall. These failures can be classified according to four failure mechanisms: 1) direct failure of weathered bedrock; 2) failure of colluvium from the impact of runoff cascading from cliff pourovers, known as the "firehose effect"; 3)

failure of saturated colluvium; and 4) combinations of these three mechanisms. A variety of geomorphic factors relating to climate, exposed lithologic strata, geologic structure, and drainage-basin morphometry play various roles in the process of debris-flow initiation. Among these factors, the exposure of shale source areas at heights greater than 100 m above the river is particularly critical in each of the four initiation mechanisms. Shales fail readily as weathered bedrock, produce abundant colluvial source material, and form slopes where colluvium collects. Shales also provide the fine particles and clay minerals essential to the stability of debris flows, enabling them to transport rapid-forming boulders up to several kilometers from tributary sources to the Colorado River.

Earlier work has investigated the statistical significance of various morphometric parameters in relation to flood magnitude, usually emphasizing drainage-basin area, mean basin elevation, and amount or intensity of precipitation (Roeske, 1978; Blakemore and others, 1994). Patton and Baker (1976) suggest that stream magnitude may also be a good predictor of flash-flood potential for small drainage basins. They argue that transient controls, such as climatic variability, also play a significant role. Shown (1970) includes all of these variables in modeling sediment transport in the southwest, as well as factors relating to surface geology and soils such as rock type, hardness, weathering, and texture.

Because it is more a sediment transport problem than a flood problem, the frequency of debris flows in Grand Canyon is well correlated with geologic factors, such as the presence of shale source-areas, particularly the Hermit Shale. The only drainage-basin variable common to all three logistic regression models (canyonwide, eastern and western Grand Canyon) is a measure of the location of the Hermit Shale. As the youngest shale strata in Grand Canyon, the Hermit Shale has the highest exposure, providing bedrock and colluvium failures with a high degree of kinetic energy. The appearance of measures of Muav Limestone in two of three models indicates that this source lithology also plays a prominent role in debris-flow production. Although an older strata which is exposed close to river level, the Muav Limestone supports the large colluvial wedges which collect on the Tonto platform. These wedges fail frequently, and are the source of many recent debris flows.

Overall, model results reflect the complexity of debris-flow

initiation in Grand Canyon. Most variables become statistically significant only in combination with other variables, indicating the interdependence and interaction of various factors in the initiation process. As large-scale morphology varies from east to west, different drainage-basin parameters dominate the process. Eastern Grand Canyon is steep-sided and narrow, with steep drainages of variable size. As a result, standard morphometric measures, such as basin area and channel gradient, become important determinants of debris-flow production. Smaller storm systems pass more easily over a narrow canyon, except where it parallels the storm track. Thus, river aspect also becomes significant in the eastern model. In contrast, western Grand Canyon is wider, with larger drainages of a more uniform size and gentler gradient and increased faulting and folding creates greater variation in the location of important source strata. As a result, morphometric and climatic variables drop out and variables representing source areas dominate the model. Discriminating statistically significant variables becomes more difficult in western Grand Canyon, and may reflect an increase in the complexity of the initiation process. However, it may also reflect the increase in variation expected within a larger geographic area.

Future work on modeling debris-flow production in Grand Canyon could focus on the prediction of the probabilities of debris-flow occurrence in the remaining 380 tributaries. Drainages with a high probability of debris-flow occurrence that have not yet had a debris-flow this century may be primed for an episode in the near future. Additionally, spatial variability of the probability of debris-flow occurrence would likely suggest other significant factors not considered in the model.

Acknowledgements

The author wishes to thank the many individuals who helped with the field and office work that made this report possible. The professionalism of the numerous guides who piloted boats for me on the Colorado River made field work efficient, safe, and fun. Thanks also to all the people who helped with the large amount of repeat photography this study required. Sara Light-Waller, Ted Melis, Dominic Oldershaw, Dave Ring, and Robert Webb performed much of the darkroom work. Chuck Sternberg drafted the illustrations. Nohl Lyons performed much of the initial GIS work necessary for the measurement of drainage-basin parameters, and Ed Holroyd, U.S. Bureau of Reclamation in Denver, Colorado, gave extensive technical help and advice with the MIPS GIS software. Steve Sutley, of the U.S. Geological Survey in Denver, Colorado, performed all x-ray diffraction analysis. Betsy Pierson, U.S. Geological Survey, provided invaluable statistical support. I also thank Vic Baker, Jim Bennett, Yehouda Enzel, Dick Iverson, Connie McCabe, Waite Osterkamp, Tom Pierson, Steve Reneau, and Kevin Scott for their review of research design and field work. Special thanks to Vic Baker and Jay Quade, University of Arizona, for their guidance and critical appraisal, and to Robert Webb and Ted Melis, U.S. Geological Survey, for making it all possible.

REFERENCES CITED

Beverage, J.P., and Culbertson, J.K., 1964, Hyperconcentrations of suspended sediment: American Society of Civil Engineers, Journal of the Hydraulics Division, v. 90, p. 117-126.

Billingsley, G.H., and Elston, D.P., 1989, Geologic log of the Colorado River from Lees Ferry to Temple Bar, Lake Mead, Arizona, *in* Elston, D.P., Billingsley, G.H., and Young, R.A., eds., Geology of Grand Canyon, Northern Arizona: Washington, D.C., American Geophysical Union, p. 1-47.

Billingsley, G. H., Jr., and Huntoon, P.W., 1983, Geologic map of Vulcan's Throne and vicinity, Western Grand Canyon: Grand Canyon Natural History Association, scale 1:48 000, 1 sheet.

Blakemore, E.T., Hjalmarson, H.W., and Waltemeyer, S.D., 1994, Methods for the estimation of magnitude and frequency of floods in the southwestern United States: U.S. Geological Survey Open-File Report 93-419, 211 p.

Dolan, R., Howard, A., and Trimble, D., 1978, Structural control of the rapids and pools of the Colorado River in the Grand Canyon: Science, v. 202, p. 629-631.

Ford, T.D., Huntoon. P.W., Billingsley, G.H., Breed, W.J., 1974, Rock movement and mass wastage in the Grand Canyon, *in* Geology of the Grand Canyon: Flagstaff, Museum of Northern Arizona, Grand Canyon Natural History Association Publication, p. 116-128.

Fowler, D.D., 1989, The western photos of John K. Hillers: Washington, D.C., Smithsonian Press, 166 p.

Graf, W.L., 1979, Rapids in canyon rivers: Journal of Geology, v. 87, p. 533-551.

Hamblin, W.K., and Rigby, J.K., 1968, Guidebook to the Colorado River, Part 1 — Lees Ferry to Phantom Ranch in Grand Canyon National Park: Provo, Utah, Brigham Young University Geology Studies, v. 15, part 5, 84 p.

Hampton, M.A., 1975, Competence of fine-grained debris flows: Journal of Sedimentary Petrology, v. 45, p. 834-844.

Hansen, E.M., and Shwarz, F.K., 1981, Meteorology of important rainstorms in the Colorado River and Great Basin drainages: National Weather Service Hydrometeorological Report No. 50, 167 p.

Haynes, D.D., and Hackman, R.J., 1978, Geology, structure, and uranium deposits of the Marble Canyon 1° x 2° quadrangle, Arizona: U.S.

Geological Survey Miscellaneous Investigations Series Map I-1003, scale 1:250 000, 2 sheets.

Hereford, R., and Huntoon, P.W., 1990, Rock movement and mass wastage in the Grand Canyon, *in* Beuss, S.S., and Morales, M., Grand Canyon geology: New York, Oxford University Press, p. 443-459.

Hereford, R., and Webb, R.H., 1992, Historic variation of warm-season rainfall, southern Colorado Plateau, southwestern U.S.A: Climatic Change, v. 22, p. 239-256.

Hirschboeck, K.K., 1985, Hydroclimatology of flow events in the Gila River Basin, central and southern Arizona [Ph.D. dissert.]: Tucson, Arizona, University of Arizona, 335 p.

Hosmer, D.W., and Lemeshow, S., 1989, Applied logistic regression: New York, John Wiley and Sons, 307 p.

Howard, A., and Dolan, R., 1981, Geomorphology of the Colorado River in Grand Canyon: Journal of Geology, v. 89, p. 269-297.

Huntoon, P.W., and Billingsley, G.H., 1983, Geologic map of Vulcan's Throne and vicinity, western Grand Canyon, Arizona: Grand Canyon Natural History Association, scale 1:48 000, 1sheet.

Huntoon, P.W., Billingsley, G.H., and Clark, M.D., 1981, Geologic map of the Hurricane Fault Zone and vicinity, Western Grand Canyon, Arizona: Grand Canyon Natural History Association, scale 1:48 000, 1 sheet.

Huntoon, P.W., Billingsley, G.H., Breed, W.J., Sears, W.J., Ford, T.D., Clark, M.D., Babcock, S., and Brown, E.H., 1986, Geologic map of the eastern part of the Grand Canyon National Park, Arizona: Grand Canyon Natural History Association Map, scale 1:62,500, 1 sheet.

Johnson, A.M., and Rodine, J.R., 1984, Debris flow, *in* Brunsden, D., and Prior, D.B., editors, Slope instability: New York, John Wiley and Sons, p. 257-361.

Kieffer, S.W., 1985, The 1983 hydraulic jump in Crystal Rapid — Implications for river-running and geomorphic evolution in the Grand Canyon: Journal of Geology, v. 93, p. 385-406.

Leopold, L.B., 1969, The rapids and pools — Grand Canyon, *in* The Colorado River Region and John Wesley Powell: U.S. Geological Survey Professional Paper 669, p. 131-145.

Major, J.J., and Pierson, T.C., 1992, Debris flow rheology: Experimental analysis of fine-grained slurries: Water Resources Research, v. 28, no. 3, p. 841-858.

Melis, T.S., Webb, R.H., Griffiths, P.G., and Wise, T.J., 1994, Magnitude and

frequency data for historic debris flows in Grand Canyon National Park and vicinity, Arizona: U.S. Geological Survey Water-Resources Investigations Report 94-4214, 285 p.

Patton, P.C., and Baker, V.R., 1976, Morphometry and floods in small drainage basins subject to diverse hydrogeomorphic controls: Water Resources Research, v. 12, p. 941-952.

Pierson, T.C., and Costa, J.E., 1987, A rheologic classification of subaerial sediment-water flows, *in* Costa, J.E., and Wieczorek, G.F., editors, Debris flows / avalanches — Process, recognition, and mitigation: Reviews in Engineering Geology, v. VII, p. 1-12.

Powell, J.W., 1875, Exploration of the Colorado River and its canyons: New York, Dover Publications, 400 p.

Rodine, J.D., and Johnson, A.R., 1976, The ability of debris, heavily freighted with coarse clastic materials, to flow on gentle slopes: Sedimentology, v. 23, p. 213-234.

Roeske, R.H., 1978, Methods for estimating the magnitude and frequency of floods in Arizona: Arizona Department of Transportation Final Report ADOT-RS-15(121), 82 p.

SAS Institute, Inc, 1990, SAS/STAT User's Guide, Version 6, Fourth Edition, Volume 2: Cary, N.C., SAS Institute, Inc., 846 p.

Sellers, W.D., Hill, R.H., and Sanderson-Rae, M., eds., 1985, Arizona Climate: Tucson, University of Arizona Press, 143 p.

Shown, L.M., 1970, Evaluation of a method for estimating sediment yield: U.S. Geological Survey Professional Paper 700-B, p. B245-B299.

Smith, W., 1986, The effects of eastern North Pacific tropical cyclones on the southwestern United States: Salt Lake City, Utah, National Oceanic and Atmospheric Administration, Technical Memorandum NWS-WR-197, 229 p.

Starkey, H.C., Blackmoun, P.D., Hauff, P.L., 1984, The routine mineralogical analysis of clay-bearing samples: U.S. Geological Survey Bulletin 1563, 32 p.

Stephens, H.G., and Shoemaker, E.M., 1987, In the footsteps of John Wesley Powell: Boulder, Colorado, Johnson Books, 286 p.

Stevens, L., 1990, The Colorado River in Grand Canyon, A guide: Flagstaff, Arizona, Red Lake Books, 107 p.

Turner, R.M., and Karpiscak, M.M., 1980, Recent vegetation changes along the Colorado River between Glen Canyon Dam and Lake Mead, Arizona: U.S. Geological Survey Professional Paper 1132, 125 p.

U.S. Water Resources Council, 1981, Guidelines for determining flood flow frequency: Hydrology Subcommittee Bulletin 17B, 183 p.

Webb, R.H., 1996, Grand Canyon, a century of environmental change: Tucson, University of Arizona Press, 273 p.

Webb, R.H., and Betancourt, J.L., 1992, Climatic variability and flood frequency of the Santa Cruz River, Pima County, Arizona: U.S. Geological Survey Water-Supply Paper 2379, 40 p.

Webb, R.H., Pringle, P.T., Reneau, S.L., and Rink, G.R., 1988, Monument Creek debris flow, 1984 — Implications for formation of rapids on the Colorado River in Grand Canyon National Park: Geology, v. 16, p. 50-54.

Webb, R.H., Pringle, P.T., and Rink, G.R., 1989, Debris flows in tributaries of the Colorado River in Grand Canyon National Park, Arizona: U.S. Geological Survey Professional Paper 1492, 39 p.

United States Department of the Interior

GEOLOGICAL SURVEY

RESEARCH PROJECT OFFICE
DESERT LABORATORY - USGS
1675 Anklam Road
Tucson, AZ 85745

December 21, 1995

GLEN CANYON ENVIRONMENTAL
STUDIES OFFICE

DEC 22 1995

RECEIVED
FLAGSTAFF, AZ

Richard Quartaroli
Glen Canyon Environmental Studies
U.S. Bureau of Reclamation
P.O. Box 22459
Flagstaff, AZ 86002-2459

Dear Richard,

Enclosed are 2 copies of a recent M.S. Thesis by Peter G. Griffiths. The report represents a major creative extension of previous ideas on morphometric controls on debris flow frequency and provides a basis for modelling sediment inputs from ungaged tributary canyons. This one is not part of my obligation to a contract mod; I am merely sending it to you for your information and library.

Yours truly,

Bob

Robert H. Webb

ENCL: Griffiths thesis